LASER-INDUCED BREAKDOWN SPECTROSCOPY (LIBS) ON GEOLOGICAL SAMPLES: COMPOSITIONAL DIFFERENTIATION AND RELATIVE HARDNESS QUANTIFICATION

by

SIPOKAZI NTOMBIZIFIKILE PANYA PANYA

Submitted in accordance with the requirements

for the degree of

MASTER OF SCIENCE

In the subject

PHYSICS

at the

UNIVERSITY OF SOUTH AFRICA

SUPERVISOR: PROF M. MAAZA

CO-SUPERVISOR: PROF B.M. MOTHUDI

FEBRUARY 2018

DECLARATION

Name: S.N. Panya panya

Student number: 58563474

Degree: MSc in Physics

LASER-INDUCED BREAKDOWN SPECTROSCOPY (LIBS) ON GEOLOGICAL SAMPLES: COMPOSITIONAL DIFFERENTIATION AND RELATIVE HARDNESS QUANTIFICATION

I declare that the above dissertation is my own work and that all the sources that I have used or quoted have been indicated and acknowledged by means of complete references.

…….. ……

Signature **Date**

DEDICATION

This thesis is dedicated to my late grandfather, Fumanekile Kleinbooi Panya panya; and my parents: Welile Alfred and Zimkhitha Gloria, Panya panya.

ACKNOWLEDGEMENTS

Firstly, I would like to thank God, through which all things are possible, for enabling me to start and finish this thesis.

I am very thankful to the University of South Africa (UNISA) for affording me the opportunity to register with a prestigious institution. I am thankful to the National Research Foundation (NRF) for their financial support.

I am very thankful to my supervisor Prof Malik Maaza and co-supervisor Dr Ahmed Galmed; I am thankful for their support, their motivation and for their efforts, patience, and time. Likewise, my acknowledgement goes to iThemba LABS for hosting me, the MRD stuff and fellows for support during the duration of my MSC. I would be amiss if I would forget to thank Dr Mthuthuzeli Zamxaka who in the very beginning inspired me and encouraged me to embark on this journey and his constant support through prayer- I will forever be grateful.

My gratitude also goes to the Council for Geosciences (Bellville) and Dr Anton Du Plessis for providing me with samples to work with. I would like to thank the UCT and Stellenbosch University geology departments for their assistance in the cutting of the samples.

I would like to thank the National Institute for Laser Enhanced Sciences (NILES), Cairo University, Egypt for receiving me and allowing me to perform my LIBS experiments in their facility, I would also like to thank them for the training they provided, guidance and support during my stay in their institution. I would also like to extend my acknowledgements to Dr John Kennedy for the PIXE experimental results.

Finally, I would like to acknowledge and express my appreciation to my families (Panya panya and Mshumpela) and friends, who supported me and encouraged me throughout this period and for their prayers.

ABSTRACT

This master's thesis is focused on the LIBS technique for compositional differentiation and relative hardness quantification of selected geological samples. The experimental part of this thesis was conducted at the National Institute of Laser Enhanced Sciences (NILES) in Cairo, Egypt where a simple LIBS system was constructed. In parallel to the experimental work, the literature review was surveyed with the aim to give a thorough view of the history, fundamentals and all the factors related to LIBS. LIBS is a developing analytical technique, which is used to perform qualitative and semi-quantitative elemental analysis of materials (solid, liquid and gas). The fast data collection and the lack of sample preparation made LIBS be an attractive technique to be used for geological samples. This study was done to improve analytical methods for geochemical analysis of samples during different exploration phases (Mining, filed analysis, etc.), as a real-time analysis method to save money and time spent in labs. For a generation of laser induced plasma, a Q-switched Nd: YAG laser operated at 10 Hz and wavelength of 1064 nm was employed on the surface of the samples. A spectrometer fitted with an intensified charge-coupled device (ICCD) was used to disperse and detect the spectrum; then fed to a computer for recording and further processing of the data. The sample set was compiled from samples collected from different areas (South Africa and Namibia). Using principal component analysis (PCA), it was found that LIBS was able to differentiate between the samples even those of the same area. The results from the LIBS technique were correlated with subsequent analysis of the same samples by Particle-induced X-ray emission (PIXE). The feasibility of relative hardness estimation using LIBS was done by measuring the plasma excitation temperature for different samples. LIBS with its advantages as an elemental analysis technique made it possible to estimate the hardness of geological samples. Based on theory and results, an analytical technique for compositional differentiation and quantification of relative hardness of geological samples is proposed.

KEYWORDS

Laser-induced breakdown spectroscopy (LIBS)

Laser-induced plasma (LIP)

Geological samples

Rocks

Compositional differentiation

Elemental analysis

Particle- Induced X-ray Emission (PIXE)

Chemometrics

Relative hardness estimation

Plasma excitation temperature

LIST OF ABBREVIATIONS

LIBS: Laser-Induced Breakdown Spectroscopy

PIXE: Particle- Induced X-ray Emission

ICCD: Intensified Charge-Coupled Device

Nd: YAG: Neodymium-doped Yttrium Aluminium Garnet

Fe Ore: Iron Ore

OES: Optical Emission Spectrometry

PCA: Principal Component Analysis

Fm: Formation

SW: Shock Waves

S/N: Signal to Noise Ratio

Si: Silicon

Al: Aluminium

Fe: Iron

Ca: Calcium

Na: Sodium

Mg: Magnesium

Ti: Titanium

Mn: Magnesium

LIBS-PCA: Laser- Induced Breakdown Spectra analysed with Principal Component Analysis

LTE: Local Thermodynamic Equilibrium

T_e: Electron Temperature

N_e: Electron Density

LIST OF FIGURES

LIST OF TABLES

TABLE OF CONTENTS

CHAPTER ONE: INTRODUCTION

In 2009, Hermon et al. described LIBS as:

"An atomic emission spectroscopy method that is non-destructive and which is proficient in the real-time elemental configuration of any substance (solid, liquid, and gas)"

Background

The roots of the LIBS technique extend back to 1960 during the invention of the laser, when the formation of plasma due to laser ablation was reported. Throughout the succeeding decades, lasers became more movable and affordable, computing also became prevalent and the spectrometers became more compact. Laser-based analysis became more attractive to various applications due to increased capacity and the affordability. Geologic applications for LIBS, as well as the prospect of using LIBS on the NASA Mars rovers, were explored in the 1990s. This was made conceivable by the application of multivariate statistical techniques to spectral analysis to derive more information from each LIBS spectrum. This ultimately lead to NASA's endorsement of LIBS for the ChemCam instrument on the Mars Science Laboratory and industrial, agricultural, military and geological applications [1].

The LIBS technique is a useful technique to analyse, detect and measure the chemical composition of a wide range of materials by spectrally analysing the light emitted from a plasma that is created from the target surface [2]. A pulsed laser beam is focused on the surface of the sample, where the laser energy is absorbed, and the material is ablated (picograms to nanograms), dissociated and ionized producing hot temperature plasma at the point of the laser focus. As this plasma cools down, de-excitation of the material occurs, forming the continuum and the atomic/ionic emission lines. A spectrometer coupled with an ICCD detector is used to resolve the light spectrally and temporally from the plasma and record emission lines of the elements present in a sample. Every element in the periodic table typically emits light in the 200-900 nm range, and the LIBS broadband spectrometer captures the photons emitted over the entire range. This resulting in a spectrum containing a complete chemical composition of a sample.

LIBS has unique characteristics that have potential to transform geo-analysis and discriminate between materials: (1) No necessary sample preparation allowing rapid analysis of thousands of samples; (2) because LIBS is a point detection technique it provides a mechanism to analyse small regions (20 – 100 μm diameter). Also allows whole rock analysis which can be obtainable by averaging the spectra taken across the surface of the sample; (3) standoff or close-in detection; (4) real-time response [3, 4]. It is important to note that the old traditional methods will not be substituted by LIBS but rather LIBS will open new opportunities for research.

In geological and archaeological remains (samples collected from the field) a small crater is produced on the surface of the samples and this is replicated on different spots on the sample for obtaining the general composition based on the LIBS study. This is done if the composition of the plasma represents that of the sample prior to the laser ablation. Furthermore, the material's physical properties (grain size, surface roughness, and inhomogeneity) affect the formation of the plasma. This causes a strong variation in the intensities of the measured spectrum [2].

The aim of this work is to use LIBS as a fast-analytical technique to differentiate between some selected geological samples and to measure their relative hardness properties. A Variety of samples were measured, the sample set was compiled from the samples collected from (1) the Gold, and Iron exploration mines in South Africa (granite and iron ore); (2) the Karoo (Prince Albert Formation (Fm) in South Africa (siltstone and dolerite); and (3) the Karas region in Namibia (granodiorite and leucogranite). The plasma excitation temperature was used to estimate the relative hardness of the samples. This study is a contribution to a long-term effort to examine the potential of using LIBS for chemical discrimination in geological materials, and the method has been validated by PIXE.

1.1. Minerals and Rocks

Minerals are naturally occurring and have organised a crystalline structure that is either composed of a single element or a compound; and fundamentally constitute soils and rocks. Minerals can be accurately identified by chemical analysis and X-ray; both these methods show the minerals' structure and composition which are the minerals' "fingerprints". However, these methods are slow, destructive and require expensive instruments [2]. Knowledge about minerals' chemical composition and their correct identification is significant in understanding the genesis and the history of a specific rock body [5].

A rock is generally composed of more than one mineral and it forms the solid part of the earth's crust. Rocks contain an inhomogeneous mixture of minerals in the form of grains and this cannot be categorised the same way as the minerals [2]. Geological rocks are classified into three groups according to how they formed: igneous (further divided into intrusive or plutonic rocks and extrusive or volcanic rocks), metamorphic and sedimentary rocks. There has been a long-standing need across many different fields of geosciences, for a real-time technique for chemical identification and chemical analysis that has not been fully met by the X-ray fluorescence spectrometry (XRF) and Raman spectrometry, whose approach have limited performance [2]. By contrast, broadband LIBS has the potential to measure all the elements in rocks, minerals, and soils in real-time with little or no sample preparation [5].

1.2. Problem Statement

Different instruments/techniques have been used for Geological samples' elemental analysis; such as XRF, XRD, Raman, PIXE, etc. Other techniques such as Vickers scale, Mohr's scale have been used for estimation of hardness properties of geological samples. But some of these techniques are invasive, destructive, univariate and time-consuming (slow).

LIBS will be employed for elemental analysis of geological samples as well as for relative quantification of the samples' hardness.

- To provide reliable, rapid and non-destructive analytical method for geological samples.
- To enhance accuracy and precision of results.
- To enhance detection limits of all elements on the periodic table (LIBS has detection limits that can range from >100ppm to <1ppm).

1.3. Research Aim

The study aims to use LIBS as a fast technique to differentiate between some selected geological samples and measure their relative hardness.

1.4. Objectives

- To determine the optimum LIBS experimental conditions and parameters essential for the precision of the results.
- To investigate elemental composition of samples using LIBS.
- To measure the plasma excitation temperature of the samples for estimation of hardness properties.

1.5. The motivation for the Study

Discrimination of materials (geological samples) including rocks is very important because rocks contain clues about the history of a location, how it has evolved over time and its provenance. Measuring their hardness properties assists in quantifying their strength and therefore their functionality. It is therefore important to have an up-to-date information with regards to these materials for research, education, and industrial purposes. Conventional geological study identification is only based on the physical assessment of a geologist and later laboratory-based analytical techniques, which are destructive and time-consuming. Some of the features of LIBS, especially rapid analysis and simple instrumental structure allows an in-laboratory and field measurement. The simplicity of LIBS brings hope for less time that is spent in labs and is also cost effective and will save money that is spent on expensive equipment. With little or no sample preparation required, there is no need for destroying the samples (which allows the use of the samples for multiple studies and further research) and the use of environmentally unfriendly chemicals to prepare the samples can be avoided. With the stand-off LIBS device, there is no need to take the sample(s) to the lab, rather LIBS can be taken to the sample, thus conserving the geodiversity.

1.6. Research Methodology

1.6.1. Research Steps

The objectives of the research will be achieved by following the steps below:

1. Collection and selection of the samples.
2. Elemental analysis using LIBS.
3. Correlation of LIBS results with PIXE.
4. Compositional differentiation of samples using chemometrics from LIBS spectra
5. Estimation of relative hardness properties of the samples using electron temperature and sample density

1.6.2. Softwares used:

1. Mechelle Software for data collection.
2. Origin Pro software for calculations and graph drawing.
3. LIBS $^{++}$ for LIBS data analysis.

1.7. Chapter layout

This study consists of four chapters and is highlighted as follows:

Chapter 1: Introduction

This chapter entails a general introduction to the subject of the research. It includes the general background of LIBS, the background of the problem, problem statement, research aim, objectives, and the significance of the research, research methodology and research content.

Chapter 2: Literature Review

This chapter includes the history and the fundamentals of LIBS. It also includes a description of the LIBS method and its principle; and the use of LIBS as an analytical technique. General applications of the LIBS and applications of LIBS for geological samples are also included.

Chapter 3: Method of Research

This chapter will elaborate on the materials that will be investigated, on the methods that will be used to process and analyse the data. It will review the parameters, type of experimental set-up needed to achieve the aims and objectives of the study.

Chapter 4: Results and Discussion

This chapter includes the results and discussion of the data. Characterisation of the results and the correlation of results recorded; ending with the conclusions and recommendations of the study.

CHAPTER TWO: LITERATURE REVIEW

"There wouldn't be any LIBS device on Mars Rover developed by NASA if LIBS were not a very robust and feasible technique"

Richard E. Russo, EMSLIBS 2013 conference, Bari, Italy

The LIBS measurement is based on the laser-induced plasma. This chapter takes an account of the literature used in understanding the concept of LIBS, the history, its fundamentals, and all other factors related to the instrument. It also includes a description of the LIBS method and its principle; the various kinds of lasers used in LIBS. Finally, general applications of LIBS and the application of LIBS in geological materials.

2.1. History and Fundamentals of LIBS

2.1.1. LIBS Description

Cremers and Randziemski, (2006) [6] describes LIBS as an atomic emission spectroscopy (AES) that sources hot vaporization, atomization, and excitation by using plasma produced by the laser.

Hermon, et al (2009) [5] describes LIBS, as a simple atomic emission spectroscopy toechnique that is proficient of real-time, and basically a non-destructive determination of the elemental composition of any substance either solid, liquid, or gas form.

Alvey, et al., (2010) [7] describes LIBS as a real-time analytical technique with potential for geochemical analysis in the field. Due to its simultaneous sensitivity to all elements, broadband LIBS spectra can be recorded with a single laser shot, providing a unique chemical "fingerprinting" of any type of material (solid, liquid and gas).

Kasem and Harith, et al., (2014) [8] describe LIBS as an analytical technique that has a variety of applicable uses for both qualitative and quantitative elemental observations.

The above-mentioned statements agree that LIBS is a method of atomic emission spectroscopy (AES) that uses laser-generated plasma as the source of vaporization,

atomization, and excitation of the sample. Elemental compositions of samples (solid, liquid or gas) are determined by making analysis for the unique light emitted by each element as “fingerprinting” of the species. The elements are identified by observing the position of the lines in the spectra. When these lines have been calibrated properly their intensity measures quantification [6].

2.1.2. LIBS History

The fifty-six years long history of LIBS is basically related to the invention and development of lasers. The milestones in the LIBS research are briefly revised in this chapter.

LIBS was developed in the 1960’s during the invention of the laser, with the idea of developing an analytical technique based on the plasma that is induced by the laser spark [6]. Amongst the other atomic emission spectroscopy (AES) techniques LIBS is becoming popular; this is due to its simple, adaptable, and low-cost equipment, and its methodical flexibility [9]. Advancing technological developments have led LIBS into the 21st century with incomparable capabilities of extracting information from its laser-induced plasma (LIP), making it possible to analyse the UV, visible and IR emissions and making it possible to detect almost all the elements in the periodic table. Simultaneous analysis of multiple elements in the targeted samples is made possible by the high-resolution broadband detection of LIBS. Additionally, it is possible to obtain information on complex samples both qualitatively and quantitatively [10].

Introduction of more advanced instruments essentially led to further intense studies of the LIBS device. A clear projection of this increase is seen beginning 1995 (fig. 2.1) and since then, there have been expanded areas of study using LIBS. In the last 20 years, there has been a continuous increase in numbers regarding the number of publications in the field of LIBS, fig. 2.1 [11].

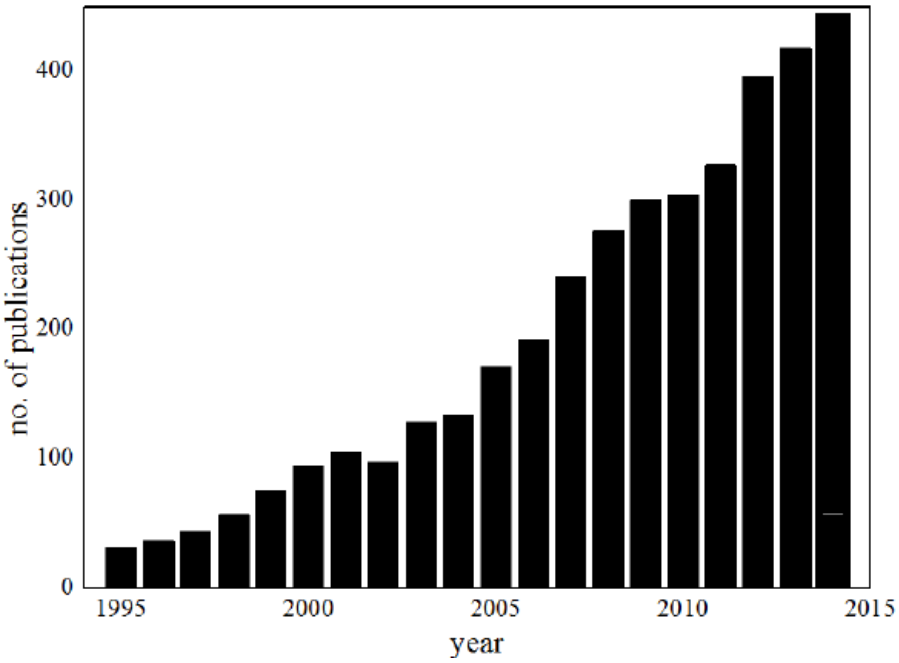

Figure 2.1: Number of LIBS publication in the last 20 years,' laser-induced breakdown spectroscopy' used as a keyword (adopted from NIST [Online]: accessed 06 October 2016)

The application of LIBS has scattered across various applications since the 90's (e.g. medical, biological, environmental analysis, cultural heritage, mineralogy, mining, space objects, archaeology, etc.). In many research groups, an understanding of the spatial and temporal evolution of plasma plume receives greater attention, together with the advancement and the optimization of the LIBS system for various applications. In the past 10 years, many review articles echoed the enormous diversity of the LIBS application. Hahn and Omenetto (2010, 2011) [12], [13] in their follow-up comprehensive studies, have reviewed fundamentals and diagnostics of LIP and the applications in which the LIBS society spread.

The plasma spectrum is the root of the LIBS measurement because it contains elemental information about the target sample. This information contained in the plasma is located at specific wavelengths, different intensities, and different line widths, and it is in the form of emission lines. Anabitarte, et al., (2012) [14] define quantitative analysis as the acquisition of relative amounts of different elements in the sample. Cremers & Randziemski (2013) [15] define qualitative analysis as the assessment of the presence of a given or unknown element(s) in a sample. A High quantitative analysis is the eventual aim of most analytical methods, which involves the determination of highly precise and accurate concentrations in a sample (e.g. ppm) or total mass. For obtaining a quantitative LIBS measurement, quite a few ways have

been proposed. One approach would be to look at the most abundant element in a species and measure its line intensity relative to the integrated intensities of the elemental emission lines. But the one conceivable way is measuring the concentration of each measurement independently, working with emitted lines and therefore making total the measurements of the intensities. For both these measurements, the spectroscopic system must be calibrated. Moreover, the most practical and most common approach for extracting quantitative information from a sample is by measuring the intensities from LIBS relative to known calibration standards. For laboratory measurements, where only one or a few elements are to be determined in approximately constant matrices, the classical calibration curve technique is probably still the method of choice, although with some reservations [16].

Tsuyuki, (2006) [17] published the first paper where they investigated and deduced that material hardness can be inferred using laser-induced plasma. Two years after this paper, Abdel-Salam et al., 2007 [18] showed that the intensity value of atomic lines of certain elements can be associated with tissue hardness. They experimentally proved and confirmed this correlation to the force of the shock waves induced by laser. The ability of a material to resists abrasion, indentation, cutting, deformation and scratching defines the hardness of a material. Vickers hardness test is a commonly used hardness testing tool; its principle is related to the measuring of an intended area to an applied load which then measures the Vickers hardness number (VHN) of the material. This instrument cannot be used as an in-situ measurement because it has specific sample requirements - such as surface finish (texture and topography) and the dimension of the sample.

For real-time and for in-situ analysis in the industry, LIBS has become one of the most effective analytical techniques, due to its repeatability and detection limits being competitive compared to other AES techniques. It has also gained its popularity in the industry because of its fast, non-demanding and robust analysis, however, due to inadequate levels of the figures of merit (i.e. accuracy, precision, detection limits) quantitative analysis using LIBS has been limited [5].

Hahn and Omenetto, (2011) [13] debated on possible ways to increase the sensitivity and detection power of LIBS. The mission is to increase the signal-to-noise ratio which gives an outcome of better detection limits results. For the material’s ablation and the

production of plasma or for the pumping the energy into the prevailing plasma plume more laser pulses can be used. The double or the multiple laser pulses which are often fixated on collinear (laser pulses shot on the sample surface from the same direction) or orthogonal (laser beams perpendicular to each other) arrangements, lead to increased LIBS signal and thus the selection of the beam path geometry is very important.

2.1.3. LIBS Principle and Measuring Parameters

Laser-induced breakdown spectroscopy is an emission spectroscopic technique in which a very short- duration pulse of energy from a high-power laser is optically focused at a point, instantaneously heating the target sample to cause vaporization and atomization of nanograms of material within a microplasma. Fig. 2.2 shows schematically the principle of LIBS (in 6 phases). The laser beam is focused onto the surface of the material that is to be analysed, radiation energy is locally coupled to the material, so the material starts to evaporate, and the vaporized material dissociates and then ionizes forming the plasma. As the plasma cools, it spontaneously emits light that is gathered and analysed by a spectrometer. Lastly, for solid materials, a crater is created. The complete process illustrated in fig. 2.2 can be repetitive with frequencies of 10Hz up to 1 kHz. The plasma has a lifetime that ranges from 0.5 -10 µs conditional on the chosen laser beam parameters, the type of material to be analysed and the surrounding ambient gas [5].

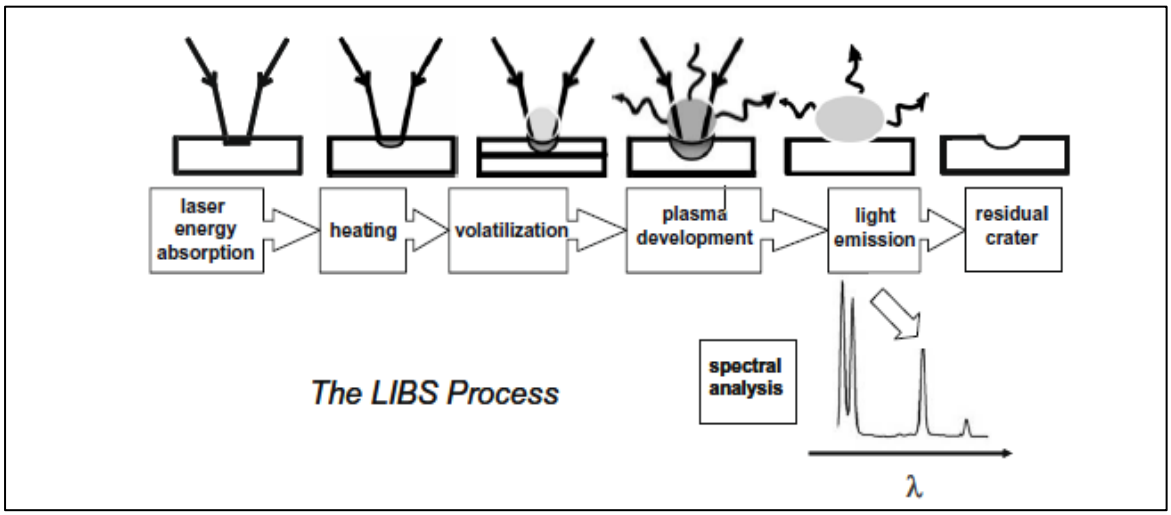

Figure 2.2: Schematic diagram of the six steps of the LIBS process (adapted from Harmon, et al., 2009).

The emission spectrum changes during the lifetime of the plasma. Fig 2.3 shows the emission spectra of the laser-induced plasma for different time delays with respect to the irradiation of the laser pulse. At time t_1 the continuous spectrum is primarily emitted, free-free (Bremsstrahlung) and free-bound (recombination) emissions cause this. At the time (t_1) only small peaks of atoms and ions intensity lines are visible with low ratio peak intensity to the continuous background. At time t_2, the plasma has cooled and there is a significant increase in the ratio peak intensity to the continuous background as well as the intensity of the line emission. Lastly, at time t_3 the temperature further decreases and so does the emission intensities.

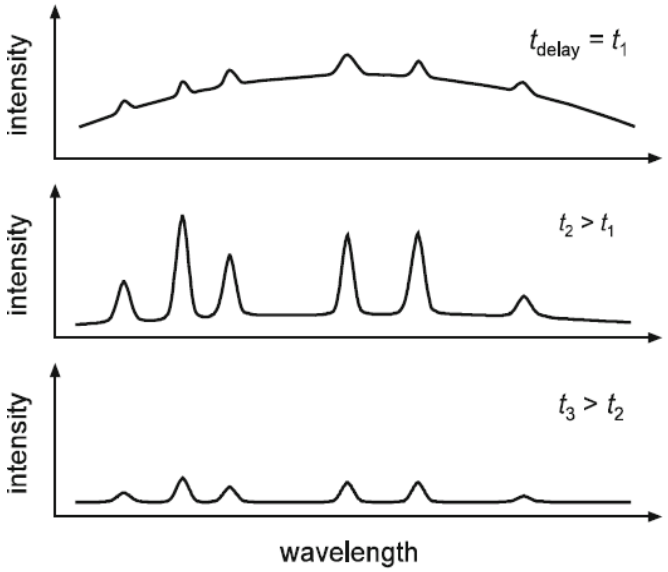

Figure 2.3: Schematic diagram of the emission spectra of the laser induced plasma for three different time delays after the laser pulse irradiation (adapted from Noll, 2002)

2.1.4. General Setup for LIBS:

LIBS measuring procedure starts with defining a measuring method or retrieving a method that has already been defined. This measuring method is defined by the selection of the measuring parameters (i.e. pre-pulse number, laser pulse energy, measuring pulses, etc.), then followed by putting the sample on the sample stand and starting the measurement. After which the spectral signals are evaluated, and the measuring results are displayed and analysed [19].

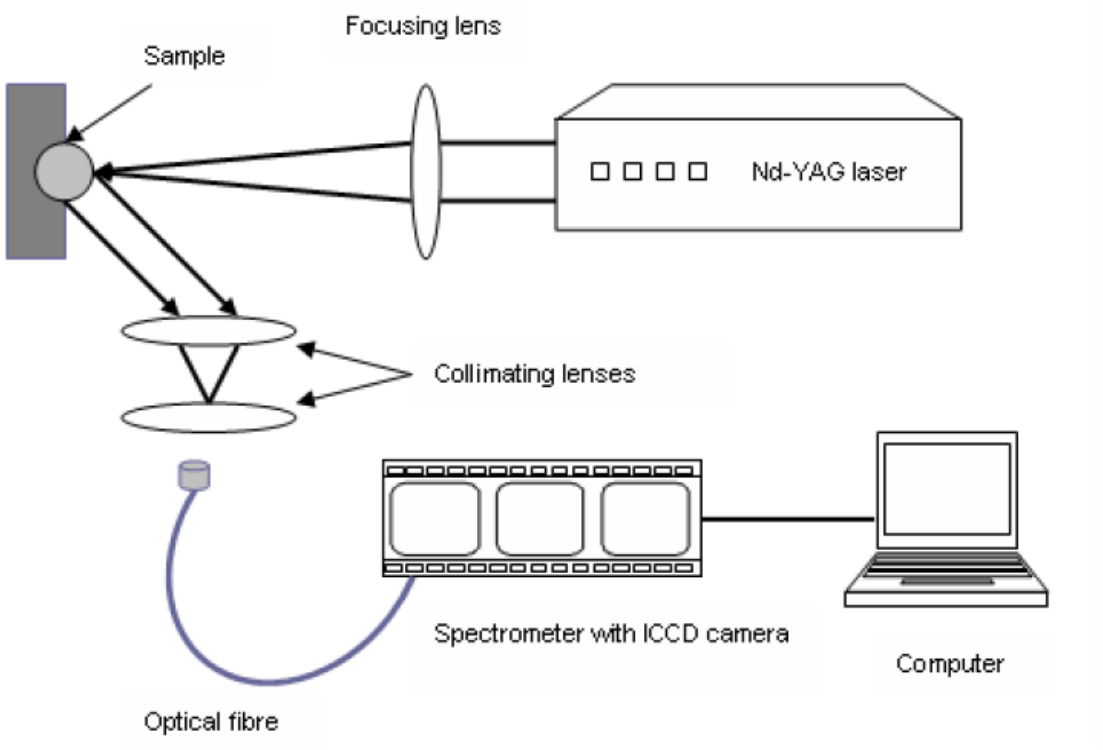

Figure 2.4: Schematic diagram of the experimental set-up used for recording LIBS Spectra (adapted from Ambushe, du Plessis & McCrindle, 2015)

The main components of this LIBS system are: a pulsed laser for the generation of the powerful optical pulses that form the micro-plasma; the lens that focuses the laser pulse on the target to be analysed; a target holder; the light collection system (off-axis parabolic mirror, plane mirror) that collects and directs the spark light into an optic fiber that transports the light to the detection system; a detection system consisting of a method to spectrally disperse the light such as the compact spectrometer/detector system; a computer to gate the detector, fire the laser, and store the spectrum [15].

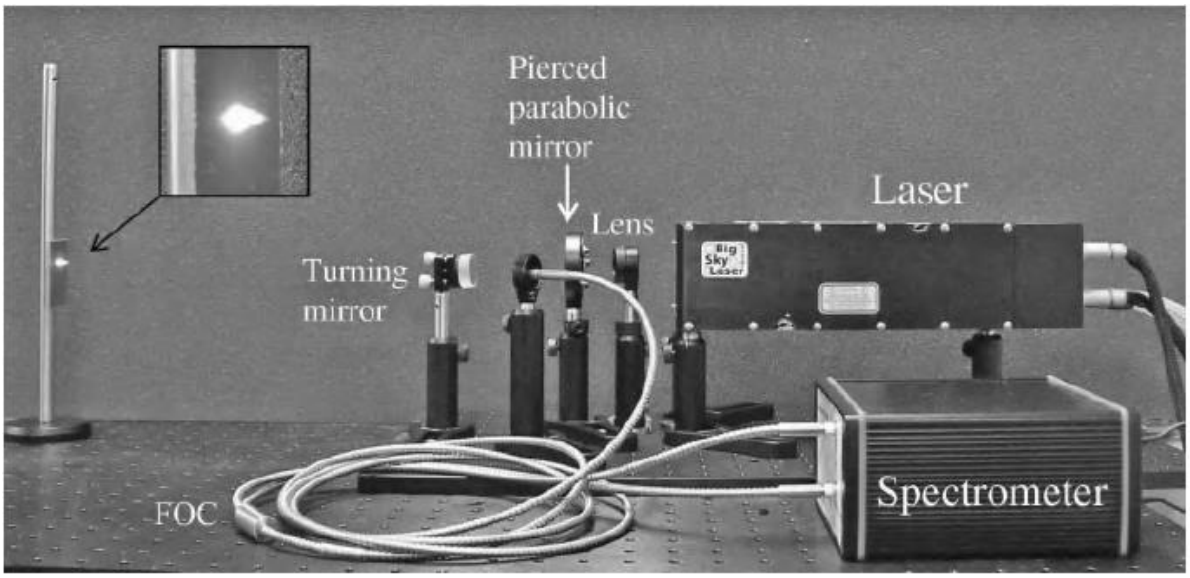

Figure 2.5: A LIBS apparatus for short stand-off distance analysis of solids. The computer and laser supply are not shown (adapted from Cremers & Randziemski, 2013).

The most common LIBS device employs a Q-switched high energy solid state Nd: YAG laser, lasing at its fundamental wavelength (1064 nm) or equipped with non-linear crystals to produce other harmonics (532, 355, and 266 nm). The lasers are usually operated at the frequency of 10 or 20 Hz, with the pulse width of ns (typically 6-10 ns) or femtosecond. Lasers (continuously pumped solid-state lasers with acousto-optical Q- switching and diode-pumped solid-state lasers with electro-optic Q-switching) with higher frequency rates (up to tens of kHz) can be used depending on the application. Any change in the laser beam parameters (pulse energy, pulse width, repetition rate and beam profile) changes the plasma properties (plasma lifetime, plasma temperature and electron density) and so the sample spectral intensity.

The pulse width is a very crucial parameter in the LIBS experiment [9], it affects the LIP. For nanosecond pulses, a LIP is produced and changes while the laser radiation continues. While for femtosecond pulses, the laser beam first transmits the energy to the material before even the ablation process starts. Nonetheless, in LIBS experiments, lasers generating shorter widths (ps or fs) are seldom used.

The heart of any LIBS measurement lies in the collection and analysis of each emission spectrum. Spectrometers have properties which are important for the adequate collection of data, such as a good resolution which can provide a minimum separation of wavelengths whereby the adjacent spectral features can be viewed as two distinct and separate lines. The second crucial factor is the width of the spectrum

that can be detected, a wider band of observation is needed when simultaneously monitoring numerous elements. There are different methods used for the spectral component of a LIBS system namely: (1) Narrow bandpass less than 1mm with a fixed-wavelength line fitter; (2) Acousto-optic tunable filter (AOTF); (3) A monochromator; (4) Spectrograph and (5) An echelle spectrograph [6]. The echelle spectrograph is predominantly used in LIBS measurements because it offers the crucial wavelength coverage ranging from 190 nm - 800nm with a high spectral resolution useful for LIBS detection. Also, the strongest emission lines of most elements in the periodic table are within the same range [20].

A detector (such as the: photomultiplier-PMT, charge coupled device-CCD, Intensified charge coupled device-ICCD, etc.) is used to detect the emission from the laser-induced plasma. These detectors have different properties and parameters and thus should be carefully chosen per application and per selected spectrometer. The most important parameter is that it should be time gated. The detectors and spectrometers are generally used in the following arrangement: (a) Paschen-Runge spectrometer and PMT or CCD line detectors, (b) Czerny-Tuner spectrometer equipped with an intensified PMT or CCD line detector, and (c) echelle spectrometer and typically the ICCD detector.

When measuring solids, the “no need for sample preparation” results in unlimited contamination of the measured surface; though with a clever design of the experiment the side effects can be avoided [9].

Today, LIBS has and is mostly studied mainly in the academic field. The standard with commercial LIBS instrument covers several industrial applications, though their performance is limited [9]. Every LIBS device is built for a specific practice and enhanced for case studies, even though the basic principles of instruments stay unchanged. Fig. 2.4 is the scheme for a basic LIBS setup that was used by Ambushe et al., (2015) [21] in their study for determination of Cr in the soil. Fig. 2.5 is a diagrammed apparatus for short standoff distance LIBS experiments.

2.2. LIBS as an Analytical Technique

2.2.1. LIBS Advantages

LIBS like any other Atomic Emission Spectroscopy (AES) method can detect all elements and has the competency for multiple element detections. Compared with conventional based AES analytical methods, LIBS has various distinct advantages. This is because LIBS forms a plasma using a focused laser beam compared to other devices such as a pair of electrodes or plasma torch. LIBS technique has a simple, fast, and real-time measuring capability. It allows in situ analysis with little or no sample preparation, requiring only optical access to the sample. It can sample all kinds of samples equally well (gases; liquids, and solids); It can sample elements (Cl, F) that are difficult to monitor with conventional AES methods, due to its good sensitivity. It can adapt to different measuring set-ups (e.g. direct analysis, fibre optic delivery, compact probe, and stand-off analysis), and finally, LIBS can be done in severe conditions that can't be done by some of the other techniques. LIBS have various setup geometries that have been developed for both short distance measurement (in which the sample is placed nearby the LIBS device) and for remote measurements (in which the sample can be a couple of meters away from the instrument). This setup allows LIBS to perform distant measurements for the hazardous materials and explosives [22].

Fibre optic delivery is also a well-known and recent way for laser delivery and plasma emission collection which also make it possible to have a compact system as well as performing stand-off LIBS analysis [23]. In the stand-off analysis, the laser is directed onto a distant sample using long optical focal length system. The achievable distance depends on the selected measuring parameters (i.e. laser pulse energy and power, an optical system, beam divergence, etc.). Analysis scenarios for the stand-off analysis range from a cm to a couple of meters [24].

2.2.2. Considerations in the use of LIBS

Sample homogeneity: One of the LIBS advantages is the capacity to analyse samples with little or no preparation. Because LIBS is a point detection method, it becomes complicated to measure non-homogenous samples, where preparation would commonly produce a homogenous sample from a non-homogenous one. Samples like gases and liquids can be supposed to be homogenous and solid materials cannot always be assumed to be homogenous; with a few exceptions for some metals and plastics, etc. In this case, the LIBS measurements can be done at various positions of the sample then the resultant spectra are then averaged out or in the case of significantly inhomogeneous samples, it may be advisable to grind and press the subsequent powder for the analysis. Although this process disregards the real-time and *in situ* analysis advantages of LIBS, it still reserves analysis ability that does not require the sample to be chemically treated [6].

Matrix effects: whereby the element signal is not the same for different samples although the element under study concentration remains the same. Matrix effect can be either physical or chemical. The physical matrix depends on the physical properties of the sample and relates to the ablation step of LIBS; where the amount of ablated element changes. Chemical matrix happens when the emission characteristics of one element are affected by the presence of another element. A typical example is seen with the signal strength of silicon in water, soil and steel, although the concentration is the same in all three matrices, the signal differs [25].

2.3. LIBS Applications

LIBS is advantageous in a variety of fields especially those which can benefit from a real-time and quick chemical investigation at the atomic level, with no preparation of samples or even in the field [14].

2.3.1. Surface Hardness

Laser-induced plasma can be employed not only as an elemental analysis technique but also as a technique used for measuring the surface hardness of solid materials (from metal alloys to calcified tissues). Abdel-Salam et al., (2007) [18] in their study of three calcified tissues, confirmed that the material's hardness is directly proportional to the shock wave (SW) and the ionic to atomic line ratio (the harder the material the

higher the SW speed and the higher the atomic to ionic line ratio of Mg). In the work by Kasem et al., (2011) [26] it was established that by evaluating calcium ionic to atomic spectral line intensity ratios in the relevant LIBS spectra, surface hardness can be estimated consequently discriminating between bones of different ancient Egyptians dynasties. Idris, et al., (2010) [27] in their preliminary study on examining the capability of LIBS technique for analysing building materials' strength, concluded that there is a correlation between surface hardness and the ionic to atomic spectral line emission ratio; and this has been associated to the repulsive force of the laser-induced shock waves.

2.3.2. Depth Profiling

LIBS is a comparatively novel technique that is being applied for characterization in layered materials for depth profiling. At fixed experimental conditions, it is reliable to investigate layered materials through depth profiling procedure. A study was done by Galmed et al, (2011) [28] on Ti (thickness of 213 nm) thin films using femtosecond laser, they could make depth profiling with a low Average Ablation Rate (AAR) of 13 nm/pulse but because of lack of energy consistency through the laser pulse cross-section (Gaussian beam profile); they were unable to discriminate between the annealed and non-annealed samples. The same group did a study where they showed that if the spectral line fulfils the LIBS spectral line conditions, then any the spectral line will fulfil the same results. Normalizing the lines improved the LIBS results to be more reproducible [28].

2.3.3. Biomedical applications

In this field LIBS has not been fully explored and there is room for new developments. LIBS can and has been used to analyse the chemical compositions and hardness estimations of biomedical materials, such as teeth, bones, nails, tissue, fluids, etc. LIBS can also detect excess or deficit of minerals in these fluids, cells and tissues. It is also possible to detect cancer cells and measure the Ca and Mg concentration in such [29].

2.3.4. Cultural Heritage and Archaeology

LIBS technique has been applied as a non-destructive technique for analysing the archaeological samples like the Roman coin [30]. Caneve, et al., (2010) [31] applied LIBS in analysing valuable paintings for determining the elemental composition and to date and authenticate the colours. Archaeology and Cultural heritage samples usually cannot be moved and are of high value. In such events chemical, analytical method prepared in the labs are needed. But a portable LIBS device that does not need contact with the sample offers a better solution, thus avoiding damage to the valuable sample.

2.3.5. Industry

LIBS technique has been used as a stand-off analysis in the nuclear reactor. This technique was used to make a spectroscopic analysis without being subjected to dangerous radiation levels in nuclear reactors [32]. Rai and Rai, (2008) [33] conducted a study on industrial waste, where they used LIBS to detect the toxic products in the wastewater. They stored and recycled the data of the elements found in the water to help them minimise the impact of the process on the environment. LIBS was also used in the renewable energy field for analysis and detection of impurities in solar cells, which helped improve manufacturing process thus producing high-efficiency solar cells. LIBS has been targeting many industries for many years, because LIBS can work at long distances, making it suitable to work in harmful environments [34].

2.3.6. Geological Samples

In a review by Qiao, et al., (2015) [35] they describe LIBS as developing versatile technique in the investigation of geological materials. LIBS technique has been used in a variety of geo-analytical applications, due to its advantages that have been discussed previously. (i.e. (i) detailed chemical spectrum; (ii) lack of necessary sample preparation to allow rapid analysis; (iii) the ability to take LIBS to the field as a portable instrument and (iv) ability to analyse 20-100 µm spot and whole rocks).

LIBS in geology has been applied for the analysis of ores, extra-terrestrial materials, marine sediment, fluid inclusions and speleothems [36]. Harmon et al., (2009) [5] and Alvey, et al., (2010) [7] conducted a study where they applied LIBS for geochemical fingerprinting for rapid analysis and discrimination of minerals. In further investigations, LIBS was used as a control in the laser removal of rocks from fossils found at the

Malapa hominin site, South Africa. Where the spectra from fossils and surrounding rocks could be used as a control signal to minimise the damage that can be caused by high-speed laser removal of the fossils from the wrapping rock [37].

Kiros, et al., (2013) [38] studied the alteration processes of the rock-hewn churches from Lalibela (Ethiopia) where they applied LIBS to measure the elemental composition of both the external layers together with the bulk rock materials that were exposed to the environmental factors.

LIBS has also been used to determine the provenance of samples (such as rubies) with a success rate of >95% [39]. LIBS technique has been used for chemical mapping (understanding chemical variations within textural context); like the work that was done in Butte, Montana for mapping a copper ore [1].

In this study, LIBS will be used to compositionally differentiate between geological samples and to measure their relative hardness properties.

CHAPTER THREE: MATERIALS AND METHODS

This chapter gives a description of the samples that have been analysed, it elaborates on the sample's preparation and analysis, LIBS experimental set-up as well as other techniques that have been used during this project.

3.1. Sample Description

A Variety of samples were measured, the sample set was compiled from the samples collected directly from (1) the Gold, and Iron exploration mines in South Africa; (2) the Karoo (Prince Albert Formation (Fm) in South Africa; and (3) the Karas region in Namibia. The samples were classified by experienced geologists. The selected samples were: siltstone, granite, dolerite, banded iron formation (BIF) - iron ore, leucogranite, and granodiorite (table 3.1).

3.2. Sample Preparation and analysis

One of the unique features of LIBS is that for various measurements such as analysis of rocks or metallic samples pre-treatment or sample preparation is not required [40].

3.2.1. Sample Collection

All the samples were collected by professional geologists in the field and were all analysed through a megascopic analysis to determine their characteristics (shown in table 3.1) and address the subsequent LIBS analysis. The samples were analysed in their natural state with no previous treatment.

3.2.2. Cutting

The samples were cut into 5mm slices (lateral cut) so they could fit into the sample holder which could hold samples up to 14 mm thick. Samples were ground using 800µm Silicon carbide (Si-C) paper, to obtain a flat surface and to eliminate asperities left from the cutting process.

3.3. Analytical Techniques

3.3.1. LIBS analysis

Geological rocks are inhomogeneous in detail because of the different mineral makeup in each sample. Thus, for each sample, the LIBS spectrum was obtained by averaging measurements accumulated from firing the samples at five various locations. On each location, the signal was integrated over 5 laser shots at the same point to obtain the bulk composition after one previous cleaning shot to remove any artefact due to handling the samples in the lab. The analysis of the emission spectra was accomplished using LIBS^{++} and origin software. The entire process from sample collection to LIBS analysis is portrayed in fig. 3.1 (flow diagram).

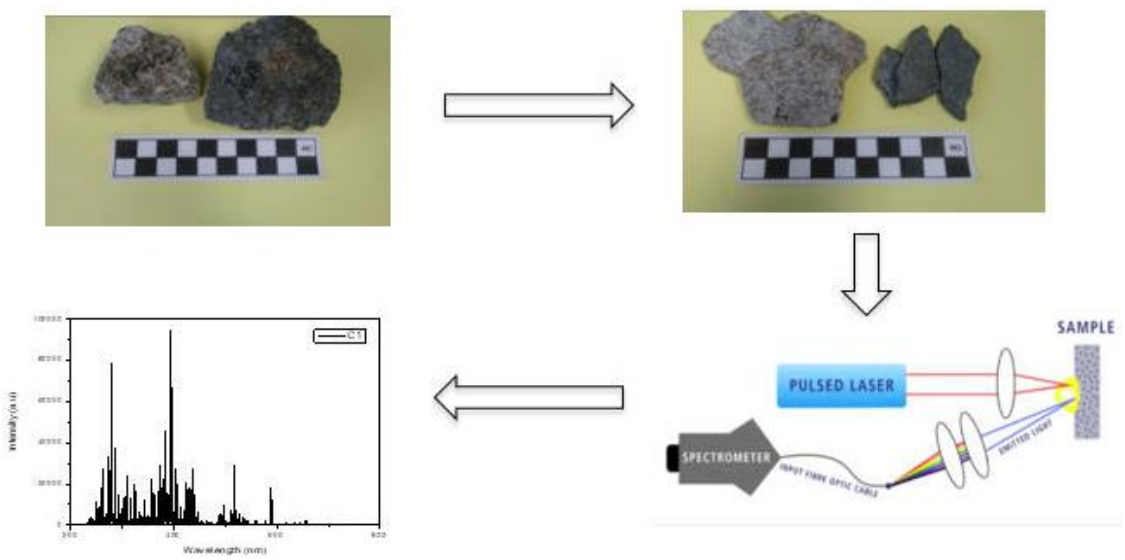

Figure 3.2: Flow diagram showing the steps from sample collection to sample analysis

Table 3.1: Rock samples analysed

Sample	Classification	Minerals	Characteristics
Siltstone	Sedimentary Rock	Clay minerals, micas, feldspar, quarts	Very fine-grained, dark grey
Granite	Igneous rock, intrusive	Major: quartz, feldspar (orthoclase feldspar). Accessory: Biotite, muscovite, amphibole, pyrite, etc.	Medium-coarse grains
Granodiorite	Igneous rock, intrusive	Major: quarts, feldspar (plagioclase feldspar). Accessory: Biotite, muscovite, amphibole etc.	Medium-coarse grains
Leucogranite	Igneous rock	Major: quarts, feldspar (alkali feldspar). Accessory: Biotite, muscovite, garnet, etc.	Medium-coarse grains
Dolerite	Igneous rock, sub-volcanic	Olivine, pyroxene, plagioclase	Dark grey, medium grains, mafic
BIF- Iron Ore	Sedimentary rock	Iron oxides: magnetite/ hematite, chert, shale	Rusty red, dark grey, silver (light grey)

3.3.1.1 LIBS Experimental Set-up

The experimental system used was based on an Nd: YAG laser source (Brio Quantel, France), emitting a laser beam of a wavelength 1064 nm. The laser energy was adjusted to be 50 mJ per pulse, while the laser pulse width was 6 ns with 10 Hz repetition rate. The laser beam was focused by a 10 cm plano-convex quartz lens. The sample was placed on X – Y – Z stage to be able to change the position of the laser spot on the sample during measurement. The distance between the sample and the lens was adjusted to be 1 mm before the focus to be sure that no breakdown takes place in the air. The laser-induced plasma plume emission was collected via a quartz optic fibre (core diameter 0.6 mm, length 1.5 m), the free terminal of the fiber was positioned at about 15mm distance from the focused laser spot at 45^{o} angle with respect to the surface normal, the other terminal was coupled to an echelle spectrometer (Mechell 7500, multichannel, Sweden).

The spectra were recorded using an intensified charge-coupled device (ICCD), (DiCAM-PRO, PCO-computer optics, Germany). The optimum time delay between the laser firing time and triggering the ICCD was determined by measuring the line intensities at different delay times. The best camera delay time was found to be 1000 ns and the gate width was 2500 ns. The obtained spectra were displayed and stored on a personal computer for further processing and analysis. The same PC was used to control the duration of the acquisition gate, as well as the delay between the laser firing time and the spectral acquisition time- fig. 3.2.

3.3.1.2. Chemometrics

In 1994, Svante Wold [41] tried to generally define chemometrics as: “how to get chemically relevant information out of measured chemical data, how to present and display this information and how to get such information into data.” Meaning that, when complex and multivariate data are acquired, chemometrics is of significant help. Chemometrics algorithms in the past decades have proved their importance in data mining and analysis of different fields (analytical chemistry, biology and economics), it can also serve for quantification and pattern recognition (classification).

The LIBS measurement generally results in bulky data sets, where a series of spectra represent each sample. Chemometrics algorithms are methods well-known for multivariate calibration and classification of large and complex datasets such as those given by the LIBS spectra. The LIBS spectra emulate the sample’s distribution based on their physical and chemical properties [41].

In this work, chemometrics was applied to find unpredicted latent variables among apparently diverse geological samples and thus differentiating between them.

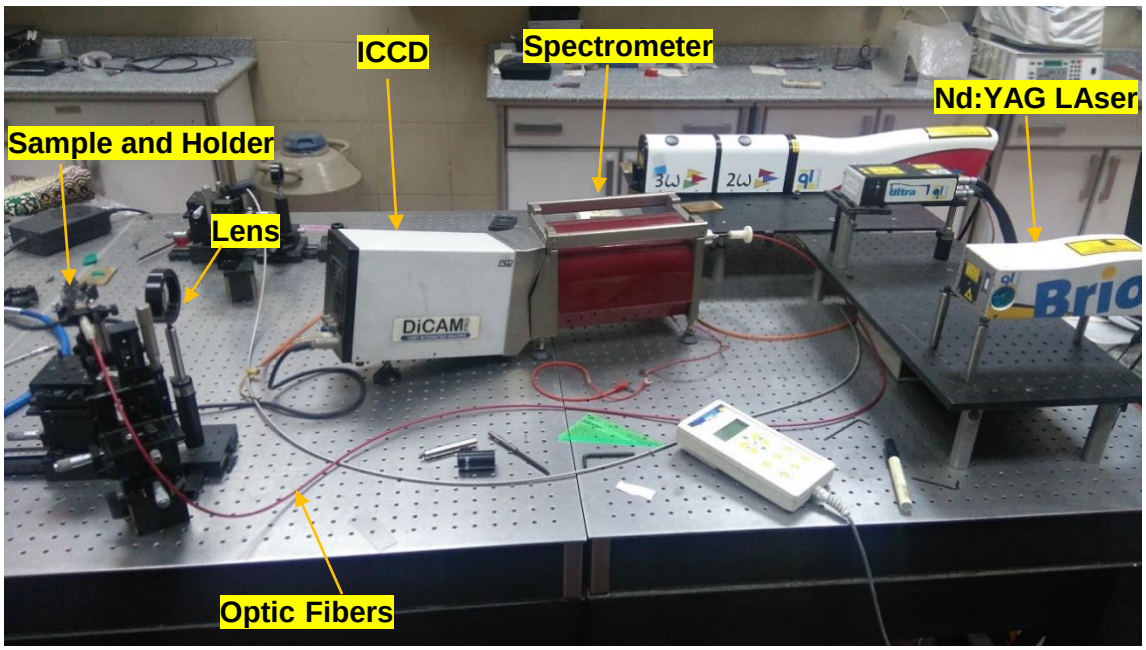

Figure 3.2: LIBS set-up.

3.3.2 PIXE

Verma, (2007) [42] discusses Particle-Induced X-ray Emission (PIXE) technique as a well-established and non-destructive analytical technique of X-ray emission that is used for fast multiple elemental analysis and simultaneous detection of many elements with high detection sensitivities in solids or liquids, even in cases where the existing sample is small. X-rays form part of the electromagnetic spectrum. The particle-induced X-rays from the sample are collected, detected and are expressed in terms of their energy in (keV) dispersive or wavelength (nm) dispersive detector systems. The detected X-rays emitted by the sample are processed in the analyser and the elements are identified by the wavelengths (qualitative), while the existing concentrations of the elements are indicated by the X-ray's intensities (quantitative).

PIXE has developed as an effective and dominant analytical technique for major, minor, and trace elemental analysis in multidisciplinary fields like biology, archaeology, environmental science, medicine, and forensic science. This technique can be used for analysing rocks, metals, ceramics, and other materials [42].

3.3.2.1 How does PIXE work?

The ultimate approach of this technique is centred on the fact that; a stable atom has electrons arranged in energy levels or shells, these different energy levels can hold a different number of electrons. When an electron is emitted from an inner shell of an atom, an electron from a higher shell drops into this lower shell to fill the hole left behind. Thus, resulting in the emission of an X-ray photon equal in energy to the energy difference between the two shells. The electrons in the inner-shell are ejected when protons or other charged particles, like He-ions, are made to impinge on the sample [42].

CHAPTER FOUR: RESULTS AND DISCUSSIONS

This chapter reports on the results obtained from the geological application of LIBS and the correlation of the LIBS results with PIXE. It also reports on the use of the LIBS spectrum on chemometric analysis (PCA) as a screening method for compositionally differentiating between the samples.

4.1. Parameter Optimization

Before discussing the results achieved in this study, it is valuable to discuss the parameter which affects the laser-induced breakdown emission and the sensitivity of the LIBS spectrometer in the rock samples. This parameter is the time delay between the laser pulse and detection of the plasma emission [43].

4.1.1. Time Delay

Fisher et al, (2001) [44]; and Martin & Cheng, (2000) [45] emphasise the importance of carefully setting of the time delay. Time-resolved LIBS spectra which were collected upon the irradiation of the dolerite and granite samples as an example of the rest of the samples since all the samples have nearly the same matrix. The experiment was done in ambient air, under atmospheric pressure over a wavelength of 200-700 nm at various delay times ranging from 500 ns – 3000 ns as shown in figures 4.1 and 4.2. Each spectrum was recorded using 5 laser shots, preceded by 1 single shot for cleaning of the sample. The optimum time delay between the laser firing time and triggering the ICCD was first determined by measuring the intensities at different delay times.

Figures 4.1 and 4.2 show the intensity-dependent spectra recorded from the samples; with a general observation that the spectrum obtained at a short delay time of 500 ns showed that the continuum intensity was very high, and the emission lines were broad. The high continuum intensity is due to the mechanisms (photoionization, radiative recombination and inverse Bremsstrahlung) that involve the free electrons, which made it impossible to obtain the information about the ions and the atoms for short delay times. The broadened emission lines are caused by the stark effect due to the electron Collisions and they indicate high electron density. However, it was noticed that at later times of the plasma expansion, the continuum emission decreased, the

emission lines became narrower and reduced indicating a decrease in electron density [46].

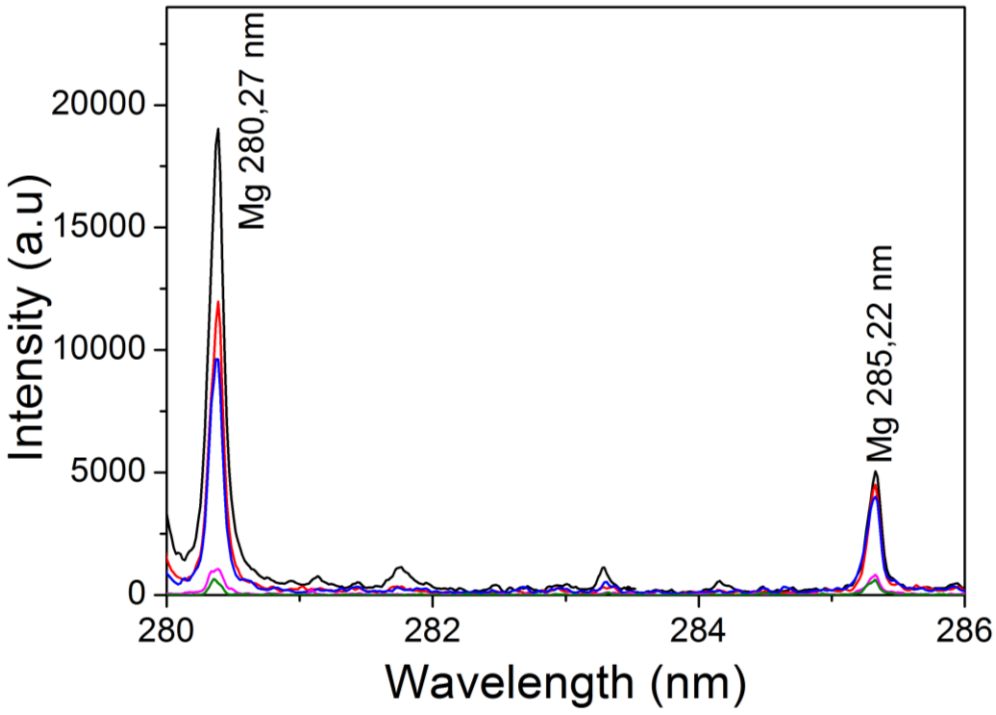

Figure 4.1: LIBS spectra obtained as a function of delay time for a granite sample. The spectrum obtained using the 1000 ns is indicated using a red colour

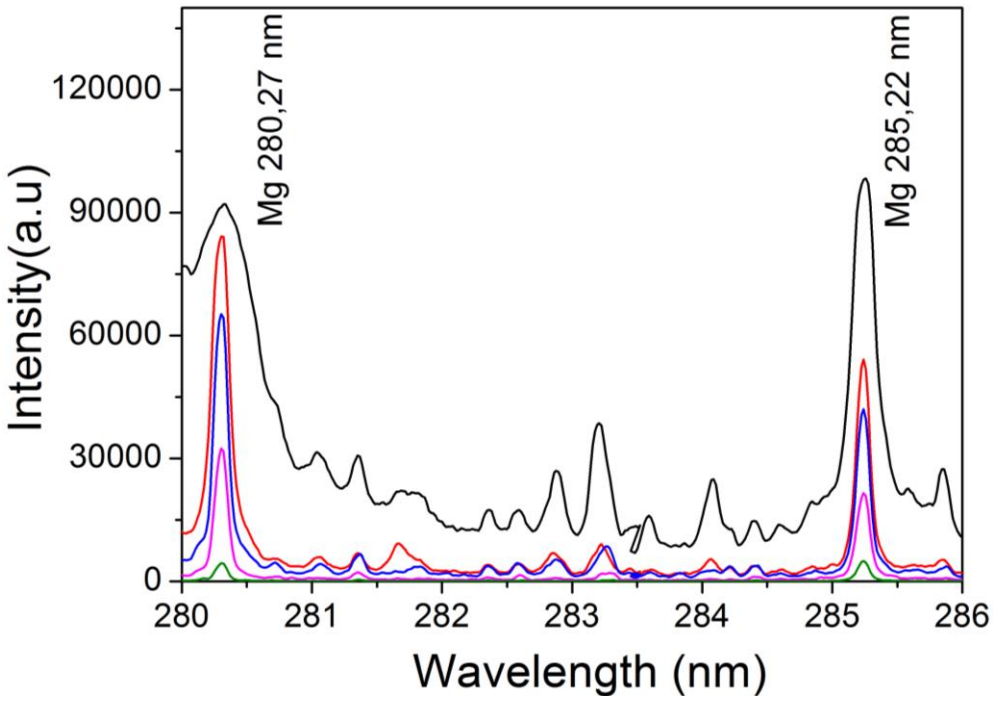

Figure 4.2: LIBS spectra obtained as a function of delay time for a dolerite sample. The spectrum obtained using the 1000 ns is indicated using a red colour

To study the behaviour of the spectral line intensities throughout the experiment, the relation between the line intensity and the delay time for the two chosen lines of magnesium and calcium are drawn in figures 4.3, 4.4, and 4.5. These figures represent the relation for the ionic and atomic lines of magnesium at 280.27 nm and 285.22 nm and of calcium at 428.9 nm and 373.6 nm (for the dolerite and granite and Fe ore samples), respectively. However, for the Fe ore sample, only the Ca ionic and atomic lines are represented because Fe ore has no Mg lines (refer to 4.2.1.1).

Fig. 4.3a represents the relation for the Mg lines at 285.22 nm and 280.27 nm in the sample dolerite. A quasi-exponential decay of the spectral lines intensities is witnessed (as the spectral line intensity decreases with increasing the delay time). However, it is important to note that the decreasing rate is not the same for different spectral lines (the intensities of the ion spectral lines are stronger in the early stages of the plasma lifetime and decay faster than the atomic lines). This is because of the recombination process of electrons and ions [47].

Fig. 4.3b depicts the same behaviour but for the Ca lines at 428.9 nm and 373.6 nm. The intensities of the lines have been found to be low and they decrease slightly at early delay time.

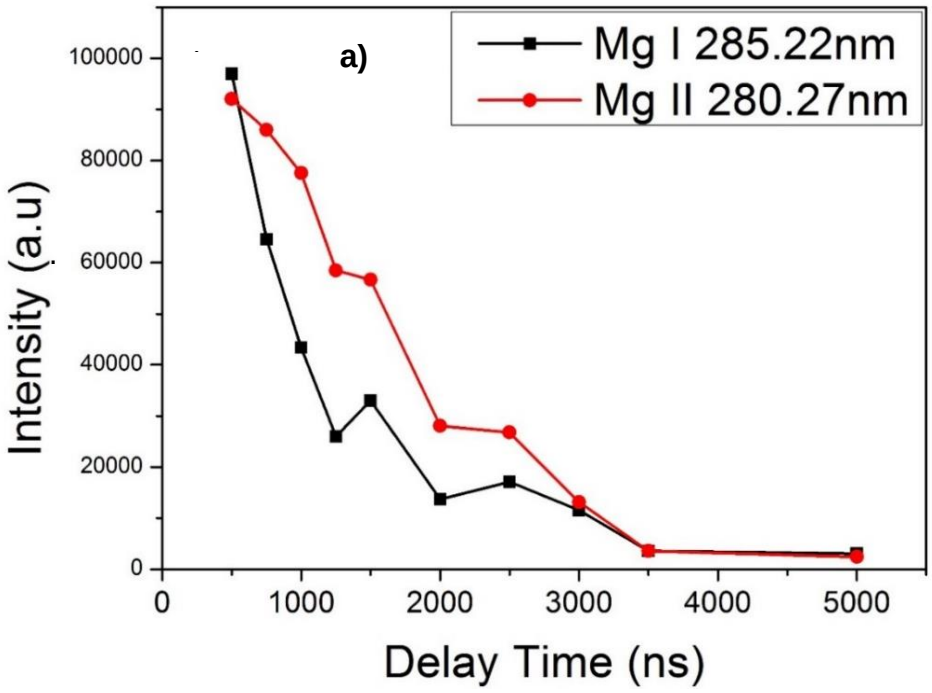

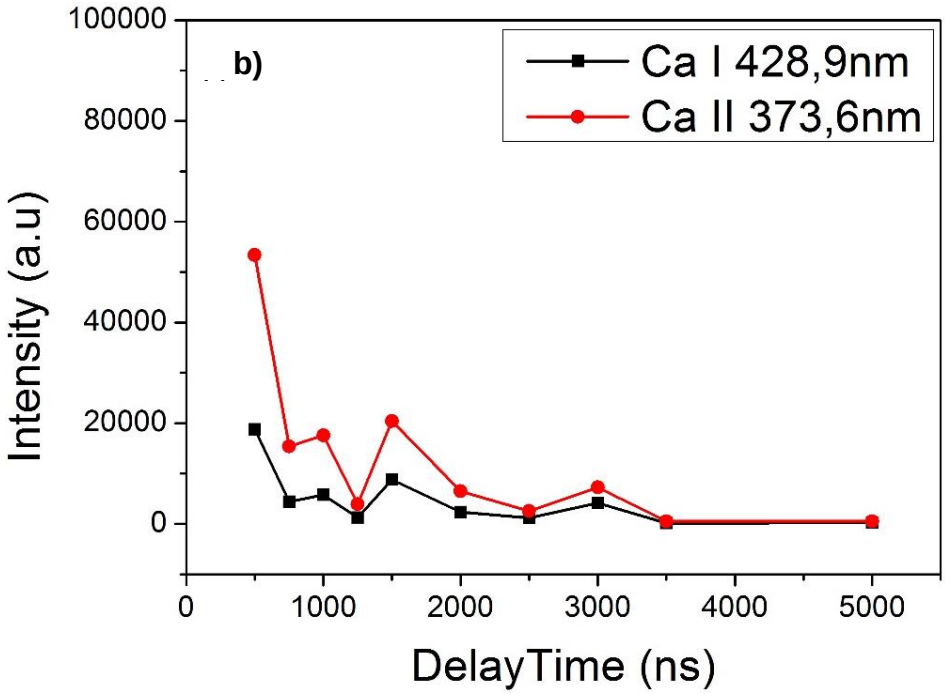

Figure 4.3: The intensity of the: a) Mg I 285.22 nm and Mg II 280.27 nm and b) Ca I 428.9nm and CaII 373.69 nm for the Dolerite sample, shown as a function of the delay time measured from the time the laser hits the surface of the sample at a pulse energy of 50 mJ.

The same ionic and atomic line intensity of Mg and Ca have been plotted for the granite in figure 4.4., in this case, the behaviour of the lines is the same. The Mg lines in fig. 4.4a, follow an almost exponential decaying pattern whilst the Ca lines in fig. 4.4b, show an irregular decaying pattern.

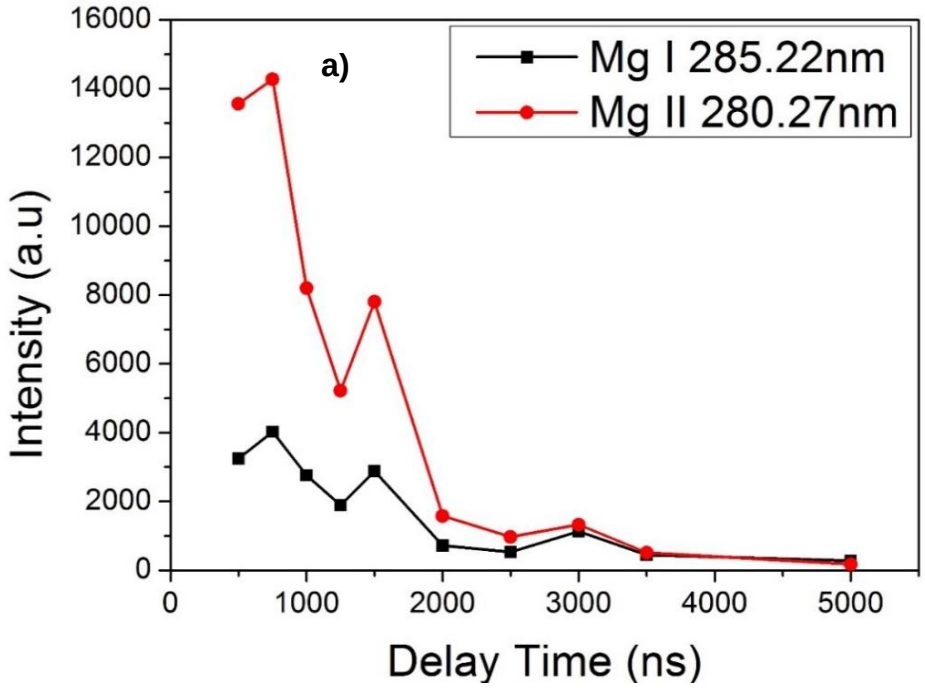

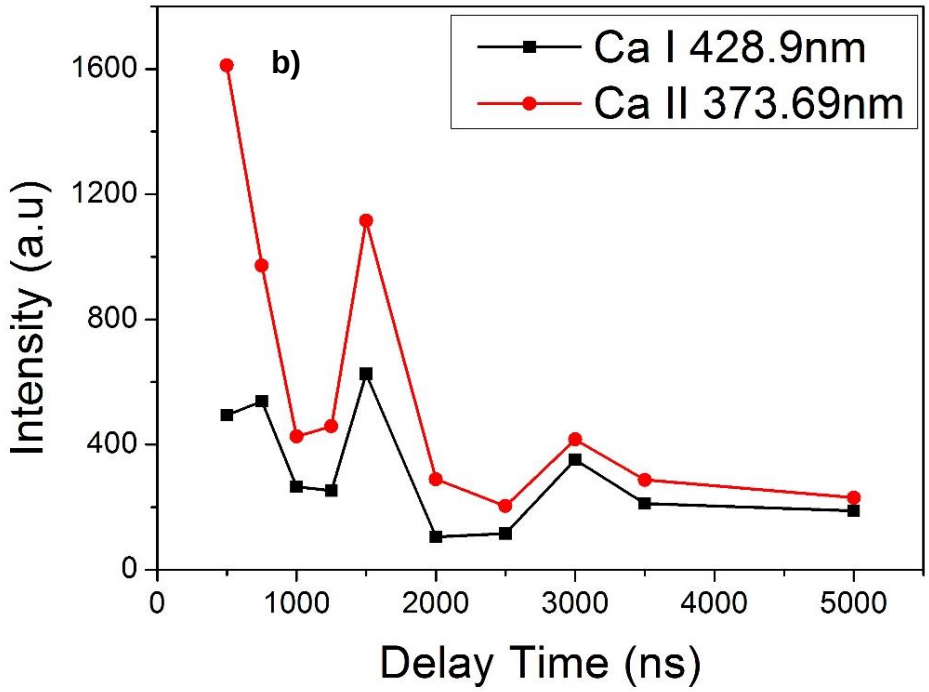

Figure 4.4: The intensity of the: a) Mg I 285.22 nm and Mg II 280.27 nm and b) Ca I 428.9nm and Call 373.69 nm for the Granite sample, shown as a function of the delay time measured from the time the laser hits the surface of the sample at a pulse energy of 50 mJ.

Similar behaviour of decreasing line intensity with increasing delay times is observed for the Fe ore sample.

Fig. 4.4 and 4.5 show that the delay time 750 ns was found to be the best point for delay time when a 50 mJ laser pulse hit the surface of the sample, however, at this point, the continuum was high while 1000 ns delay time was the first point with less continuum and separate emission lines. It was observed that the spectral line intensity decreased with increasing the delay time (quasi-exponential decay of the spectral line intensities) this is because, at the initial stages of the interaction of the laser pulse with the sample, an early intense continuum was emitted close to the surface of the target corresponding to the emission from the hot and dense plasma. As the plasma cools and expands away from the target, this results in self-absorption around the colder regions of the plasma. [48].

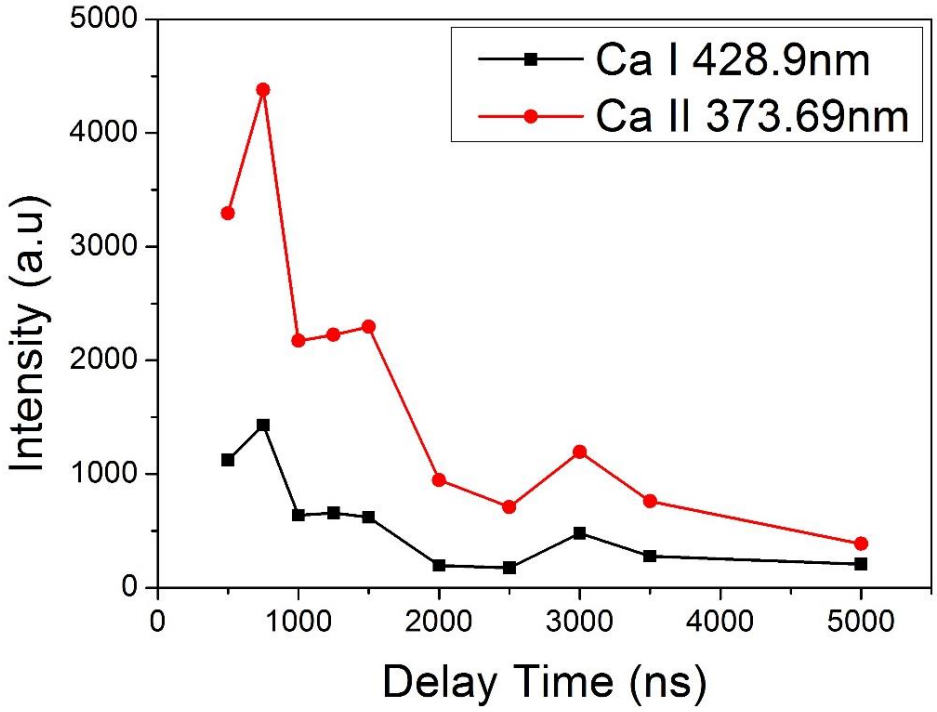

Figure 4.5: The intensity of the Ca spectral lines (Ca I 428.9nm and Call 373.69 nm) for the Fe ore sample, shown as a function of the delay time measured from the time the laser hits the surface of the sample at a pulse energy of 50 mJ.

4.1.2. Fulfilment of the LTE Conditions

To confirm if the chosen delay time was the best, it was required to confirm that the Local Thermodynamic Equilibrium (LTE) conditions were fulfilled. In doing so, both the electron density (N_e) and the plasma excitation temperature (T_e) ought to be calculated.

4.1.2.1 Electron Density (N_e)

From studying the Stark broadening of a well-isolated line in the plasma emission, the electron density can be estimated using the equation [49]; [50].

$$\Delta\lambda_{1/2} = 2\omega N_e/10^{16}$$

Where $\Delta\lambda_{1/2}$ and ω are the FWHM of a Stark-broadened line and the electron impact parameter respectively. The H_α line is the best line to be used for the calculation of N_e [51]. The values of calculated N_e are shown in table 4.1.

Table 4.1: The values of T_e, N_e and McWhirter equation values.

Sample	Slope	T_e (K)	N_e (Cm^{-3})	McWhirter value
Dolerite	-2.25E-04	6386.92	1.34E+17	4.68E+15
Fe ore	-2.57E-04	5599.935	1.53E+17	4.38E+15
Granodiorite	-6.61E-04	2175.151	1.24E+17	2.73E+15
Leucogranite	-4.49E-04	3205.263	1.22E+17	3.31E+15
Granite	-3.19E-04	4514.535	1.22E+17	3.93E+15
Siltstone	-1.83E-04	7842.924	1.37E+17	5.19E+15

4.1.2.2 Excitation Temperature (T_e)

To determine the excitation temperature (T_e), the Boltzmann plot method from the LIBS spectral line intensities is used. In this method, the populations of the excited states follow a Boltzmann distribution, and their relative emissivity (I_{mn}) can be given by the equation [52], [53].

$$\ln(\lambda_{ik} I_{ik}/g_k A_{ik}) = \ln(N(T)/U(T)) - E_k/k_B T_e$$

Where λ_{ik} and A_{ik} are the wavelength and the transition probability of the transition between the two levels k and i, respectively. g_k and E_k are the statistical weight and the energy of the excited level k. k_B is the Boltzmann constant, U(T) is the partition function and N(T) is the atomic or ion density. Then, by drawing the Boltzmann plot (Fig. 4.6), the excitation temperature can be estimated by the relation

$S = -1/(T_e)$, where S is the slope.

The excitation temperature T_e was estimated from the emission intensity of the atomic Ti spectral lines listed in table 4.2. The wavelengths, statistical weights and transition probabilities of these lines are found in Griem, [54].

Fig. 4.6 shows the Boltzmann plots for the Ti I line for the samples under study while the values of the excitation temperatures are listed in table 4.1.

Table 4.2: Ti I spectral lines used for calculating T_e.

element	ion	wavelength (A^0)	E_k (cm^{-1})	A_{ki}	g_i	g_k
Ti	1	3729.82007	26803.42	0.427	5	5
Ti	1	3752.86011	27025.65	0.504	9	9
Ti	1	3981.76001	25107.42	0.376	5	5
Ti	1	4981.72998	26910.71	0.66	11	13
Ti	1	4991.06982	26772.96	0.584	9	11
Ti	1	5173.75	19322.99	0.038	5	5
Ti	1	5192.97998	19421.58	0.0349	7	7
Ti	1	5210.39014	19573.97	0.0357	9	9
Ti	1	5223.64014	36013.57	0.135	5	5
Ti	1	5648.58008	37824.75	0.13	7	9
Ti	1	5662.16016	36351.43	0.147	9	11
Ti	1	5866.45996	25643.7	0.04	5	7
Ti	1	5953.16992	32013.53	0.0679	11	13
Ti	1	5965.83984	31914.28	0.0664	9	11
Ti	1	5978.56006	31829.97	0.0662	7	9

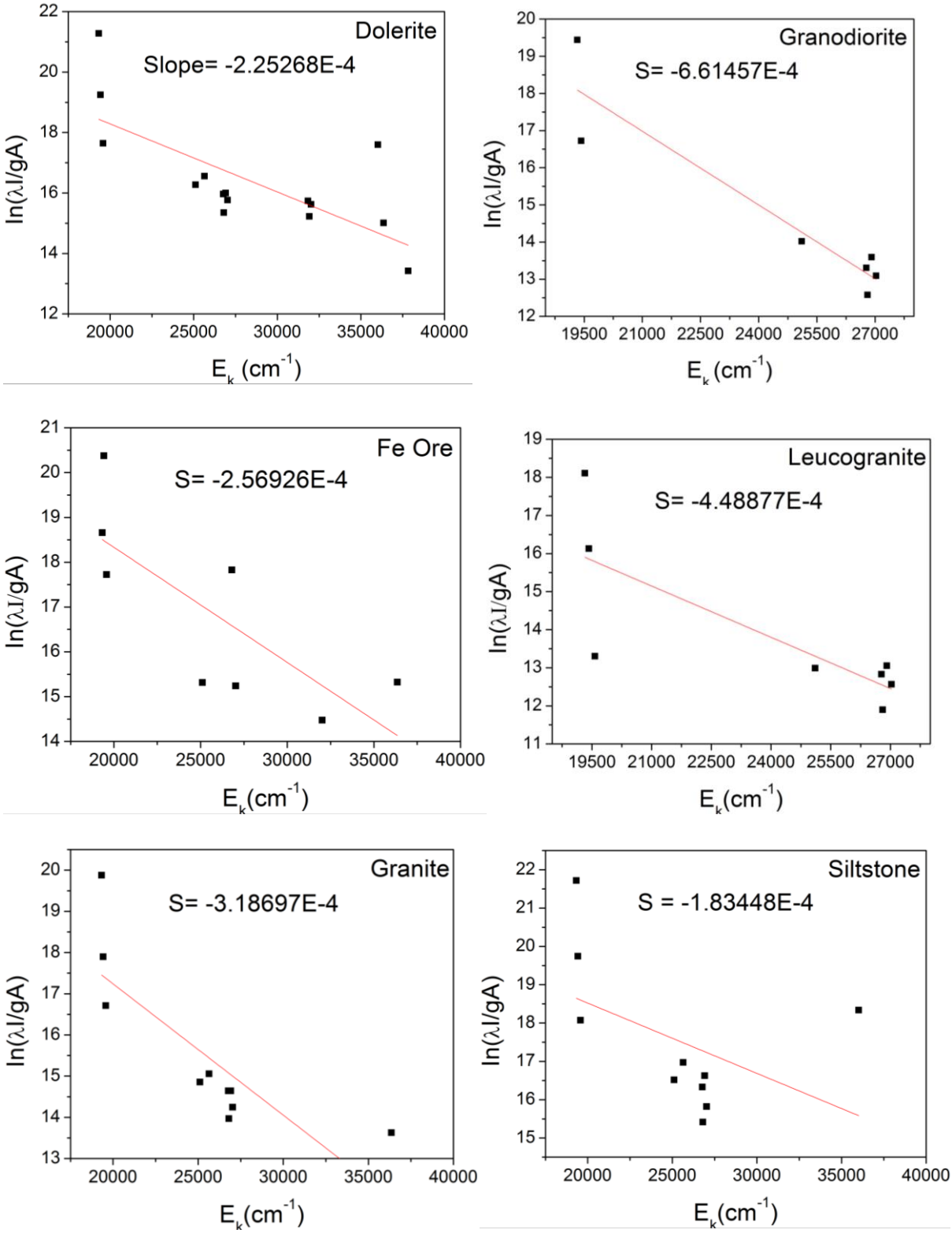

Figure 4.6: Boltzmann plot for the samples under study.

4.1.2.3 McWhirter Criterion

For the plasma to be in LTE, both the atomic and ionic energy levels should be populated and depopulated predominantly by collisions rather than by radiation. For this to happen, the electron density must be high enough to ensure a high collision rate. This was defined by the McWhirter criterion [55] where he stated that:

$N_e \geq 1.6\times10^{12}\ T_e^{1/2}\ \Delta E^3$

Where ΔE (eV) is the largest energy transition for which the condition holds (ΔE = 3.32 eV) and T_e (K) the plasma excitation temperature.

Table 4.1 (that also lists the values of the McWhirter equation) clearly shows that the values of the N_e are much higher than the values of the McWhirter equation which can be a sign that the LTE is fulfilled.

4.2. Compositional Differentiation

LIBS has been applied for several types of geomaterial analysis, including qualitative analysis and semi-quantitative analysis of element's concentrations or ratios [56]. Each LIBS spectrum contains information on the concentration of most elements in the periodic table, and that is considered the greatest potential based on the LIBS technique [57].

4.2.1. Analysis of Rock Samples

4.2.1.1. LIBS

A typical laser induced emission spectra from 6 selected samples (dolerite, iron ore, granodiorite, leucogranite, granite and siltstone) recorded in the 200–700 nm region is depicted in figures 4.7 - 4.12. The spectra were recorded for 5 accumulated laser shorts, at a laser energy of 50 mJ per pulse and a time delay of 1000 ns. To compare the compositions of the samples all the line intensities were normalized on the Carbon line 247.86 nm. Typical examples of measured spectra from the rocks with the most intense lines are shown in fig 4.7 to fig 4.12. The spectral lines of the elements studied are listed in Table 4.3. These spectral lines were identified using the NIST atomic database for neutral and ionized elements and the table of Spectral Lines of Neutral and Ionised Atoms [58]. The elements under study are the most abundant elements in the Earth's crust which are: Si, Al, Fe, Ca, Na, Mg, Ti and Mn [2]. The compositional

analysis was carried out by measuring the relative variation of line emission intensities from the elements between the different samples, selecting different emission lines to represent the corresponding elemental concentration of each element [5]; [21].

Table 4.3: Spectral line characteristics *[59]*.

Element	line (nm)	E_k (cm^{-1})	g_i	g_k	A_{ki} (s^{-1})
Si (I)	288.32	40991.884	5	3	$2.1X10^8$
Al (I)	308.20	32435.453	2	4	$5.87x10^7$
Fe (I)	275.00	44511.812	2	2	$4.85x10^5$
Ti (I)	498.17	26910.709	11	13	6.60x107
Ca (I)	422.67	23652.304	1	3	$2.18x10^8$
Na (I)	589.60	16956.17025	2	2	$6.14x10^7$
Mg (I)	285.25	35051.264	1	3	$4.91x10^8$
Mn (I)	403.10	24802.25	6	8	$1.7x10^7$
C (I)	247.87	61981.82	1	3	$2.8x10^7$

To compositionally differentiate between the six selected samples (table 3.1) an effective approach was used to locate the specific wavelengths (table 4.3) of major elements within the broadband LIBS spectrum. It is important to mention that other emission lines due to other elements do exist within these regions, however for this work the objective was to measure the abundant elements of the earth's crust.

In fig.4.7a, lines of Fe 275.00 nm, Mg 285.25 nm and Si 288.20 nm were detected in dolerite. In fig. 4.7b, Al 308.32 nm was identified. In fig. 4.7c, show the Mn line at 403.10 nm. Fig. 4.7d, a line corresponding to Ca 422.67 nm was detected. In fig. 4.7e, the Ti line at 498.23 nm was identified. The well-known doublet of Na (588.99 nm and 589.59 nm) is shown in fig 4.7.

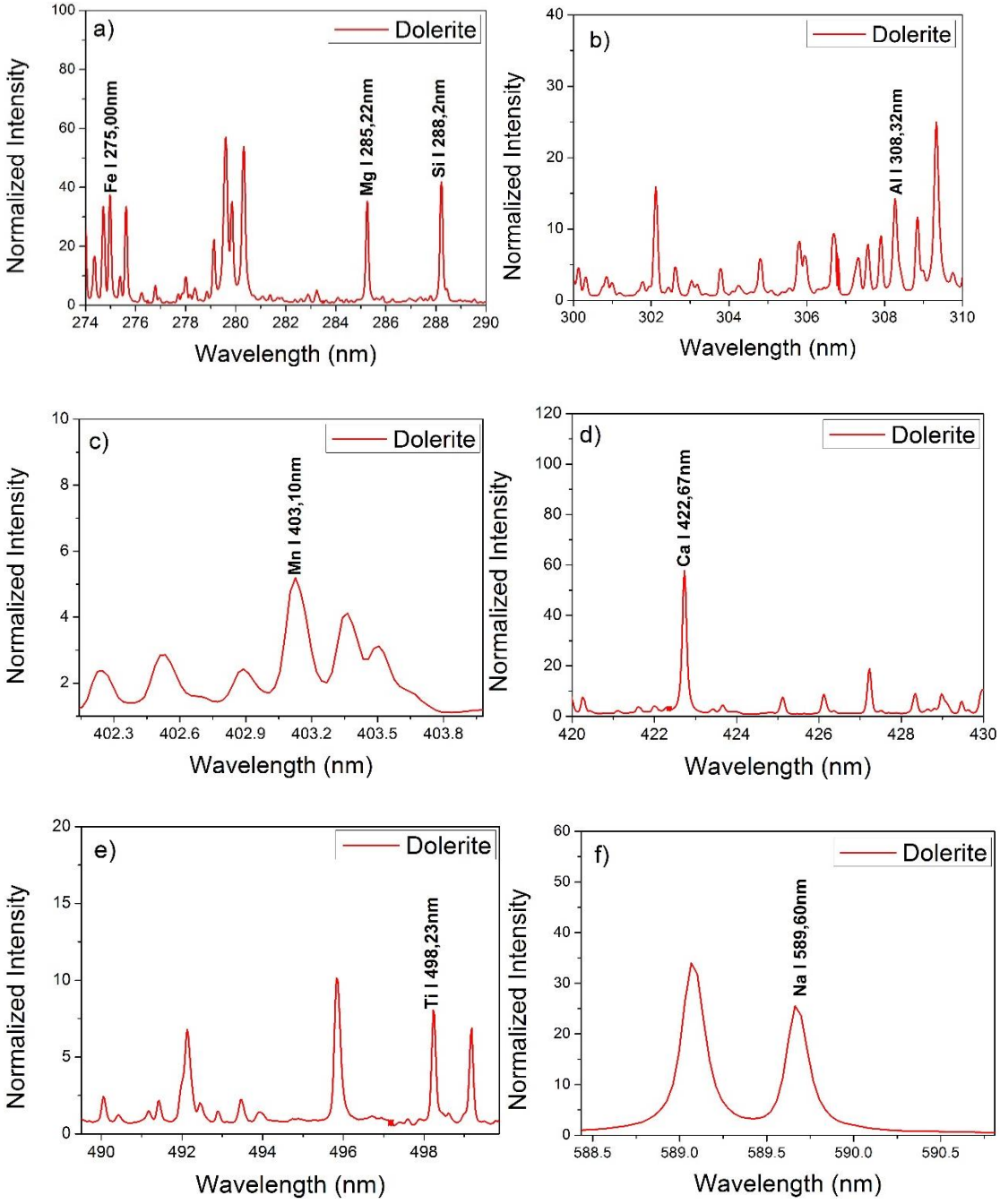

Figure 4.7: Typical LIBS spectra of the Dolerite sample recorded in the: a) 247-290 nm, b) 300-310 nm, c) 402-403 nm, d) 420-430 nm, e) 489-499 nm and f) 588-590 nm region. Emission peaks due to different elements present in the sample are indicated on the spectra

In fig.4.8a, lines of Fe 275.00 nm and Si 288.20 nm were detected, and it is important to note that the line Mg 285.25 nm was not documented in the iron ore sample. In fig. 4.8b, Al 308.32 nm was identified. In fig. 4.8c, show the Mn line at 403.10 nm. Fig. 4.8d, a line conforming to Ca 422.67 nm was identified. In fig. 4.8e, the Ti line at 498.23 nm was not identified. In fig. 4.8f, the well know doublet of Na (588.99 nm and 589.59 nm) nm was identified.

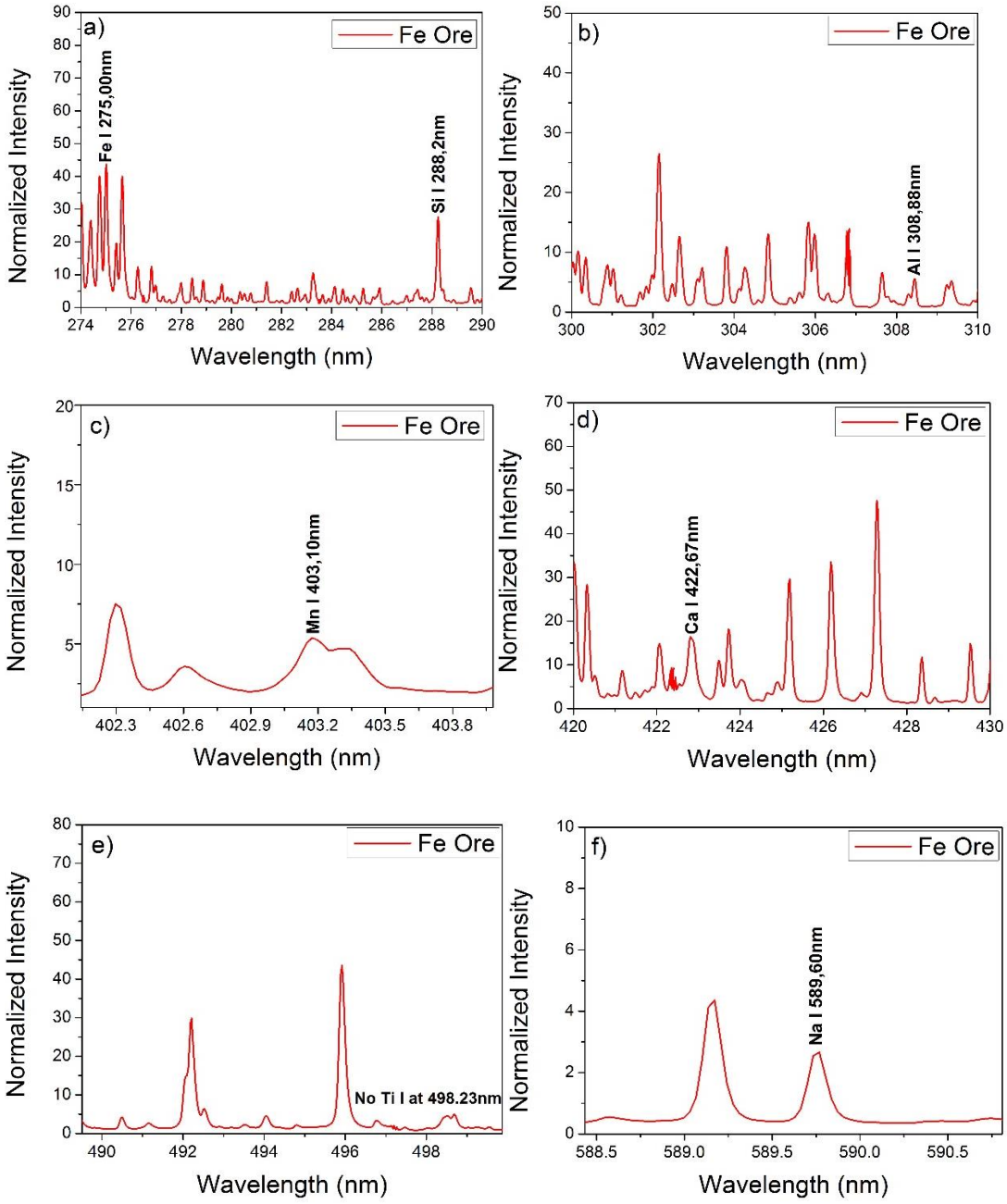

Figure 4.8: Typical LIBS spectra of the Fe ore sample recorded in the: a) 247-290 nm, b) 300-310 nm, c) 402-403 nm, d) 420-430 nm, e) 489-499 nm and f) 588-590 nm region. Emission peaks due to different elements present in the sample are indicated on the spectra.

In fig. 4.9a, it could also be seen that the presence of the lines Fe 275.00 nm, Mg 285.25 nm and Si 288.20 nm were identified in granodiorite. In fig. 4.9b, Al 308.32 nm was identified. In fig. 4.9c, show the Mn line at 403.10 nm. Fig. 4.9d, a line corresponding to Ca 422.67 nm was identified. In fig. 4.9e, the Ti line at 498.23 nm was identified. Also, the well know doublet of Na (588.99 nm and 589.59 nm) was identified (fig. 4.9f).

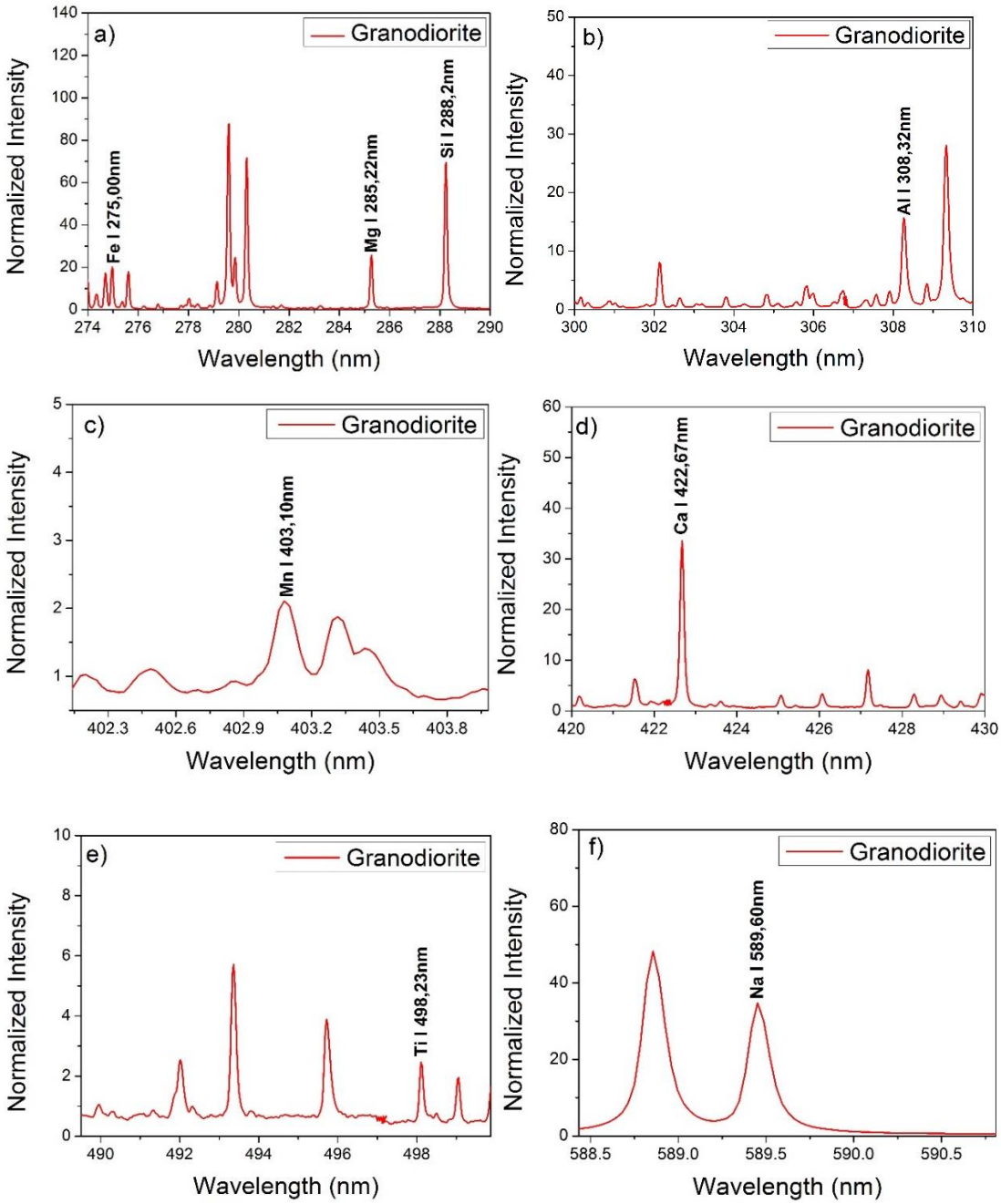

Figure 4.9: Figure 4.7: Typical LIBS spectra of the granodiorite sample recorded in the: a) 247-290 nm, b) 300-310 nm, c) 402-403 nm, d) 420-430 nm, e) 489-499 nm and f) 588-590 nm region. Emission peaks due to different elements present in the sample are indicated on the spectra.

Fig. 4.10 shows that the spectra from leucogranite contains, Fe 275.00 nm, Mg 285.22 nm, Si 288.20 nm (fig. 4.10a); Al 308.32 nm (Fig. 4.10b); Mn 403.10 nm (fig. 4.10c); Ca 422.67 nm (fig. 4.10d); Ti 498.23 nm (fig. 4.10e); and the famous Na (588.99 nm and 589.59 nm), (fig. 4.10f nm).

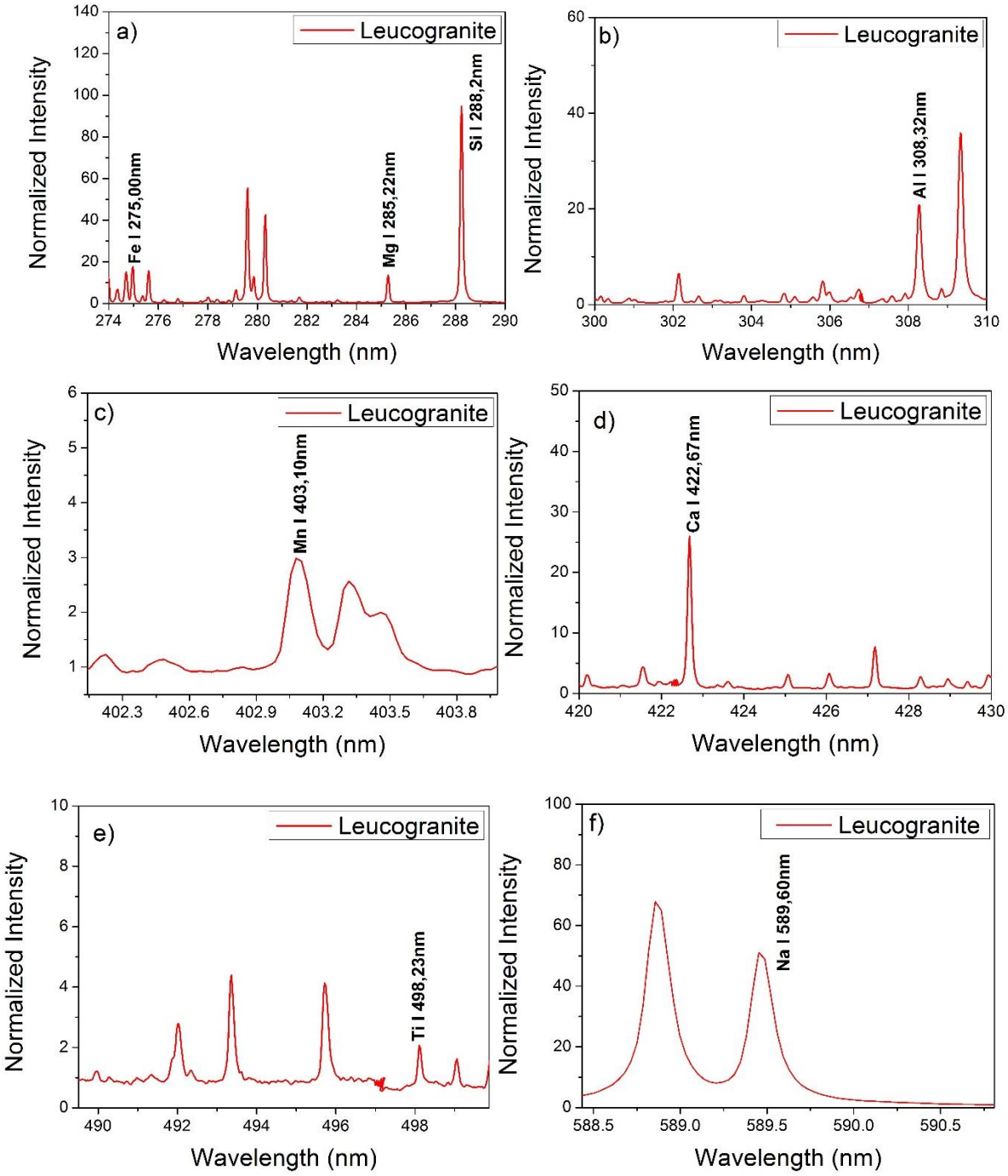

Figure 4.10: Typical LIBS spectra of the leucogranite sample recorded in the: a) 247-290 nm, b) 300-310 nm, c) 402-403 nm, d) 420-430 nm, e) 489-499 nm and f) 588-590 nm region. Emission peaks due to different elements present in the sample are indicated on the spectra.

Moreover, Granite (fig. 4.11) exhibited lines from Fe 275.00 nm, Mg 285.22 nm, Si 288.20 nm (fig. 4.11a); Al 308.32 nm (Fig. 4.11b); Mn 403.10 nm (fig. 4.11c). Furthermore Ca 422.67 nm (fig. 4.11d); Ti 498.23 nm (fig. 4.11e); and the Na (588.99 nm and 589.59 nm), (fig. 4.11f).

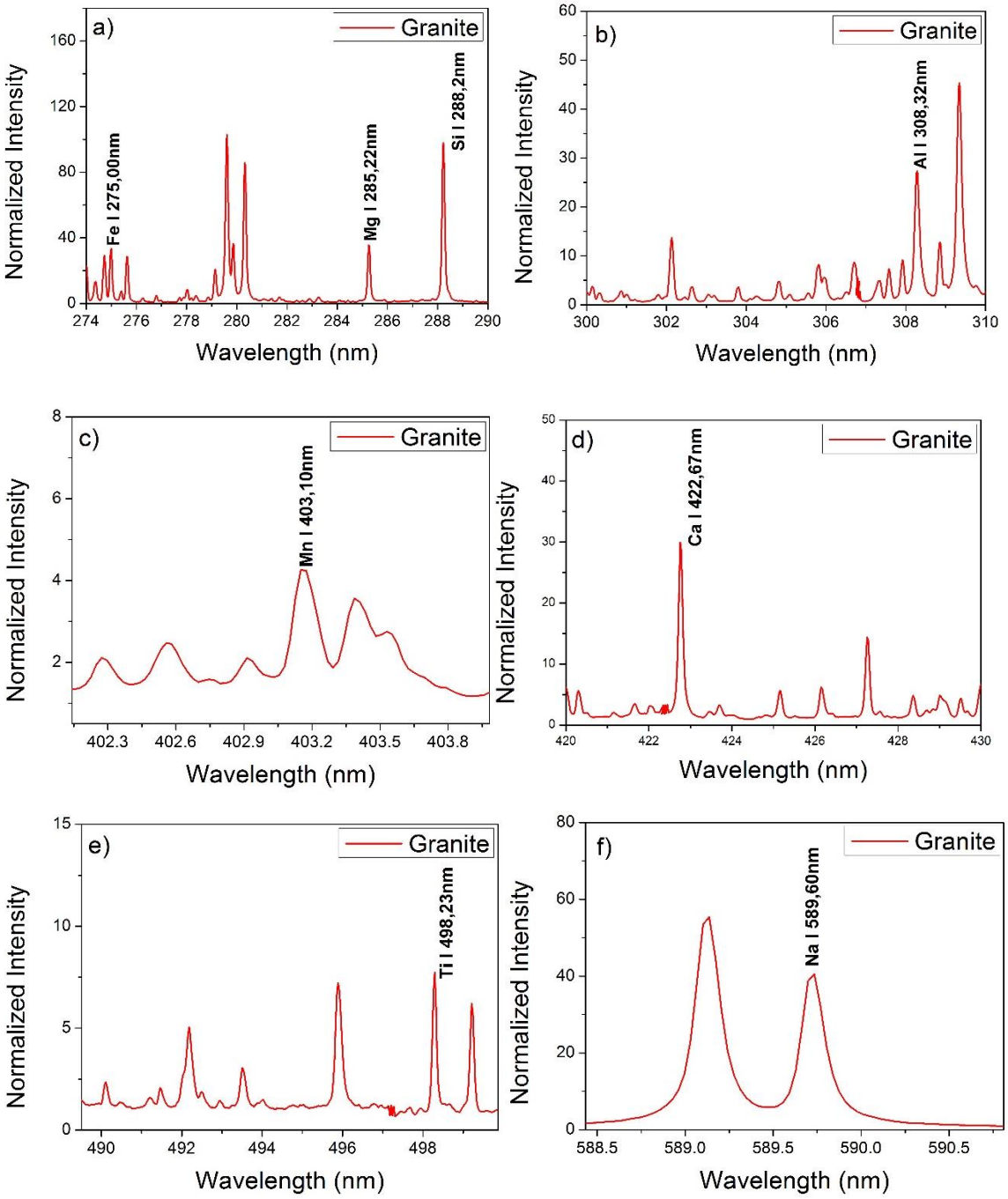

Figure 4.11: Typical LIBS spectra of the Granite sample recorded in the: a) 247-290 nm, b) 300-310 nm, c) 402-403 nm, d) 420-430 nm, e) 489-499 nm and f) 588-590 nm region. Emission peaks due to different elements present in the sample are indicated on the spectra.

The measurements on siltstone allowed us to determine the presence of Fe 275.00 nm, Mg 285.22 nm, Si 288.20 nm (fig. 4.12a); Al 308.32 nm (Fig. 4.12b); Mn 403.10 nm (fig. 4.12c). Additionally, Ca 422.67 nm (fig. 4.12d); Ti 498.23 nm (fig. 4.12e); and the famous Na doublet – Na (588.99 nm and 589.59 nm), (fig. 4.12f) nm were also detected in the siltstone.

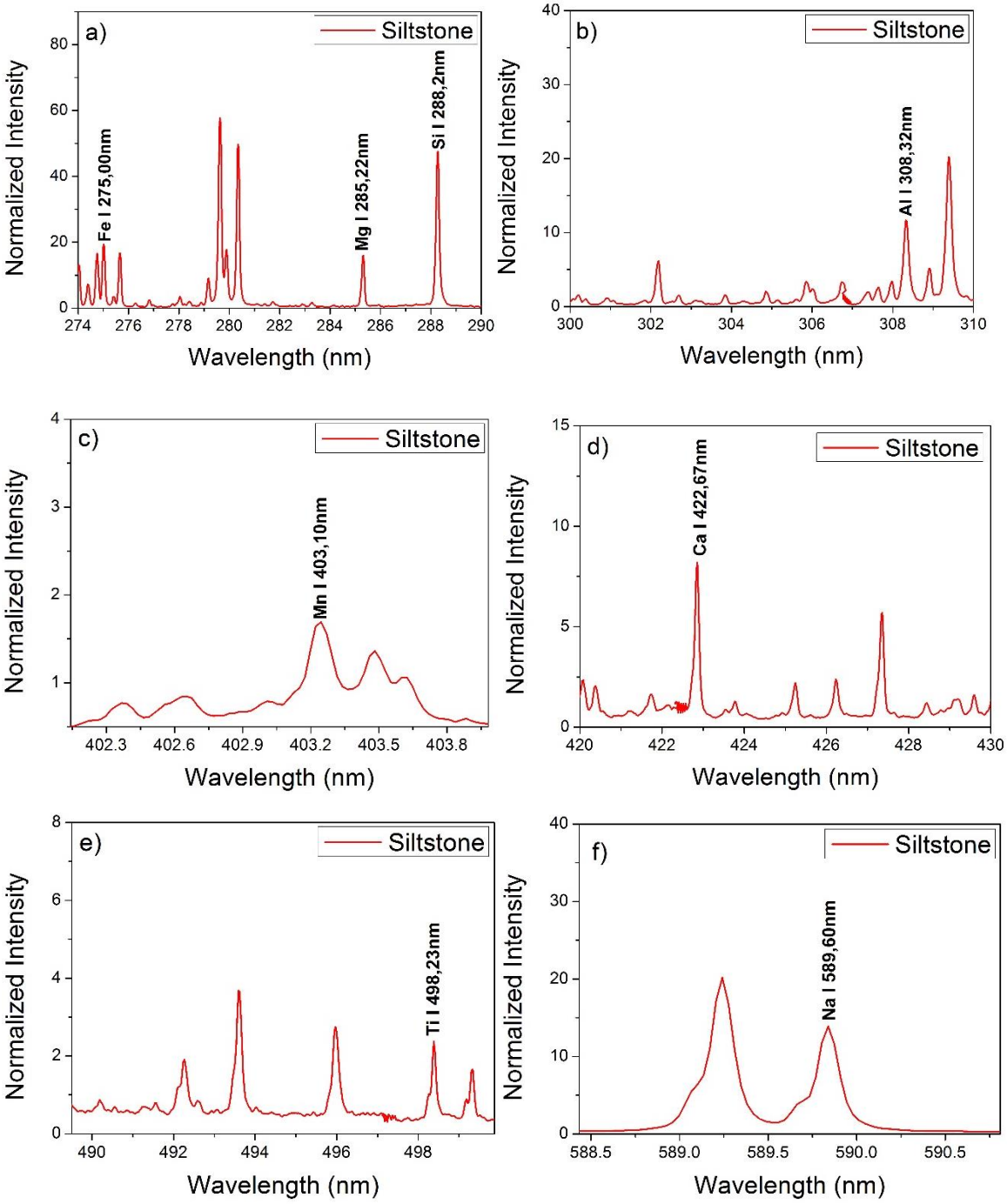

Figure 4.12: Typical LIBS spectra of the siltstone sample recorded in the: a) 247-290 nm, b) 300-310 nm, c) 402-403 nm, d) 420-430 nm, e) 489-499 nm and f) 588-590 nm region. Emission peaks due to different elements present in the sample are indicated on the spectra.

The variation of elements found in the samples is due to the primary chemical difference between the rocks, resulting in a different bulk composition of each sample. The relatively high emission intensity of Si in the samples is an indication of deposition of aluminosilicates (minerals composed of aluminium, silicon, and oxygen) in the samples. The difference in the distribution of the of Ca, Mg, and Na emission lines in some samples (sedimentary rocks, refer to table 3.1) may be that the rocks are controlled by clay minerals [38].

The Fe ore sample was devoid of Mg [7]. This is manifest because Mg has identical ionic charges and similar radii to that of Mn and due to their similar charge density, they can readily substitute for each other in iron minerals [60]. Furthermore, to support this statement [61] mentioned that the relatively low Mg content could be the result of the larger ionic radius of Mg and thus make it difficult to fit into the crystalline structure of the Fe ore; or it could be a simple reflection of lower concentrations of the Mg element in the carbonate protore. [38], state that the availability of the Na line in the samples indicates that the samples contain the mineral feldspars.

As it was reported earlier in chapter 2 (2.2.1), one of the many advantages of LIBS is that it is a simple and robust techniquel, with the ability to detect most of the elements in the periodic table. In this study, LIBS has provided the possibility of detecting low and high atomic number elements in the different geological samples thus making it possible to qualitatively analyse the samples [62].

4.2.1.2. Particle- Induced X-ray Emission Spectrometry (PIXE)

Particle Induced X-ray Emission (PIXE) was used to validate the LIBS results for semi-quantitative measurements. PIXE is a technique for multi-element analysis which provides an absolute determination of the concentrations of elements in the sample. PIXE has been established as a highly sensitive technique to study trace elements in materials [63], [64] and [65].

PIXE experiments were carried out using the 3 MV accelerator at Institute of Geological and Nuclear Sciences Ltd. The measurements were performed under high vacuum conditions in the chamber. The samples (iron ore, granite, granodiorite and leucogranite) along with reference materials were mounted in the automatic sample holder. A beam of 2.5 MeV protons with a beam current of 5-7 nA impinged on the target mounted normal to the beam. The total accumulated charge for each sample was 10 micro-Coulomb. Characteristic X-rays generated by the sample were detected by a Si (Li) detector with a 25 micron Be absorber (det.1). To improve the detection limit for heavy Z elements, such as Cu, Zn, Pb and Cd, a second X-ray detector was covered with a 25-micron Al absorber (det.2). Data were collected from the two detectors simultaneously. The PIXE spectra were analysed with GUPIX software [66] to determine the elemental concentration values.

In the previous chapter (3.3.1) it was mentioned that the geological samples are inhomogeneous in detail because of their mineral makeup in each sample. Thus, for PIXE, 13 points on each sample were measured for the concentration of each element in the respective sample. Also considering the most abundant elements in the earth's crust (table 4.1) compositional analysis using PIXE was carried out by measuring the concentration of these elements. Table 4.4 illustrates the elemental concentrations that were detected by PIXE.

Table 4.4: Concentrations (ppm) of elements in geological samples analysed by PIXE

Sample	Mg	Al	Si	Ca	Ti	Mn	Fe
Fe Ore	38760,71	7360,929	151306,4	201,8093	54,92214		173447,4
Granite	40934,69	34744	117796,8	4273,469	4449,462	603,1962	68926,15
Grano	60573,3	57394,7	173181,1	10866,1	1417,11	358,9	33387,1
leuco	56167,63	40695,13	156641,1	2066,813	582,8009	539,6875	12154,05

Si and Fe emission lines were detected in the Fe ore sample (figure 4.13), Fe element has the highest concentration compared to Si. In the granite sample (Figure 4.14) concentration of Si, Fe, Ca, Ti and Mn were identified. In granodiorite (figure 4.15) Fe, Si, Ca, Ti and Mn concentrations were detected. Lastly for leucogranite sample (figure 4.16) concentrations of Si, Ca and Fe were detected.

On qualitative bases, it was found that LIBS results agree reasonably well with the results measured using PIXE which is a good indicator that the LIBS is a useful technique for the rapid qualitative analysis of geological samples as well as other solid samples. However, it is important to note that PIXE has limitations with measuring elements that have less than 20 atomic weight (such as Na, Mg, Al, Si, etc.) and for this reason, it was noticed that some of the elements identified with LIBS could not be measured with PIXE [67].

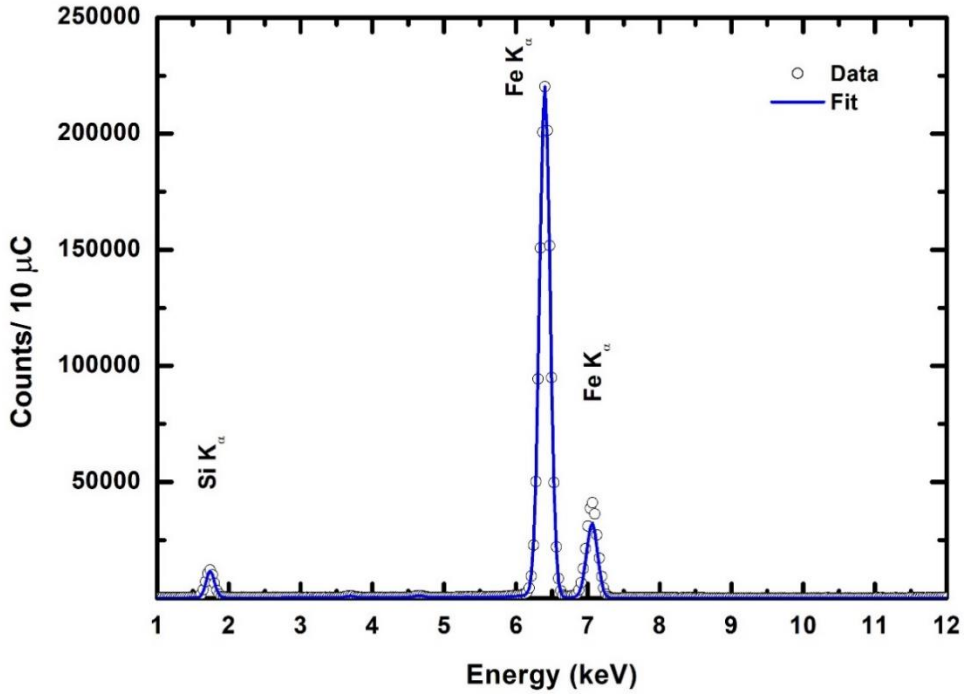

Figure 4.33: PIXE spectrum indicating the detected elements in the Fe Ore sample.

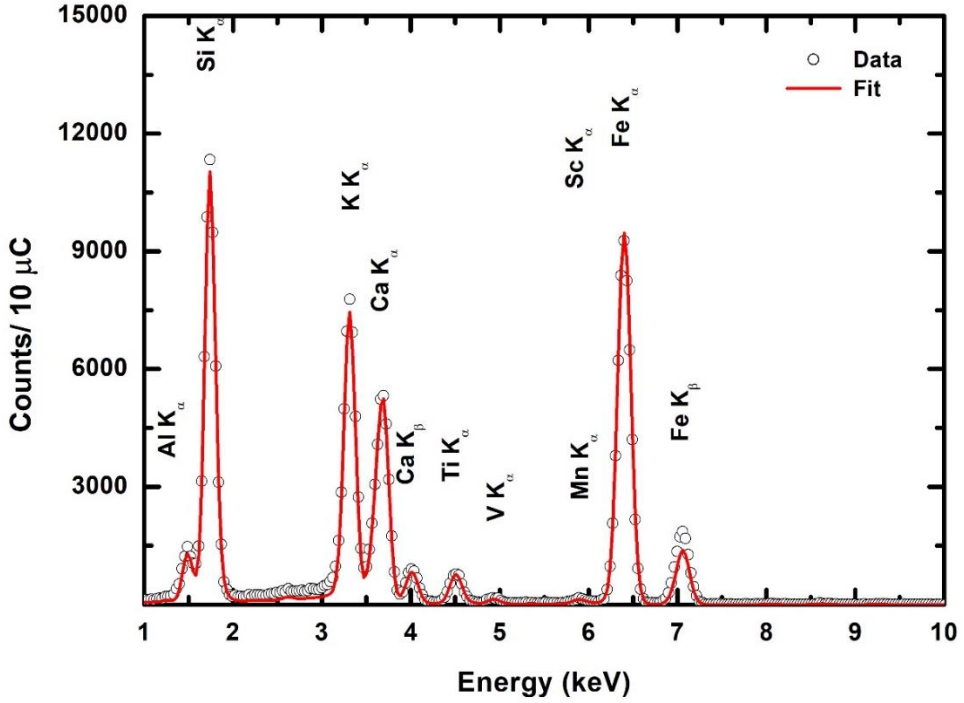

Figure 4.14: PIXE spectrum indicating the detected elements in the granite sample.

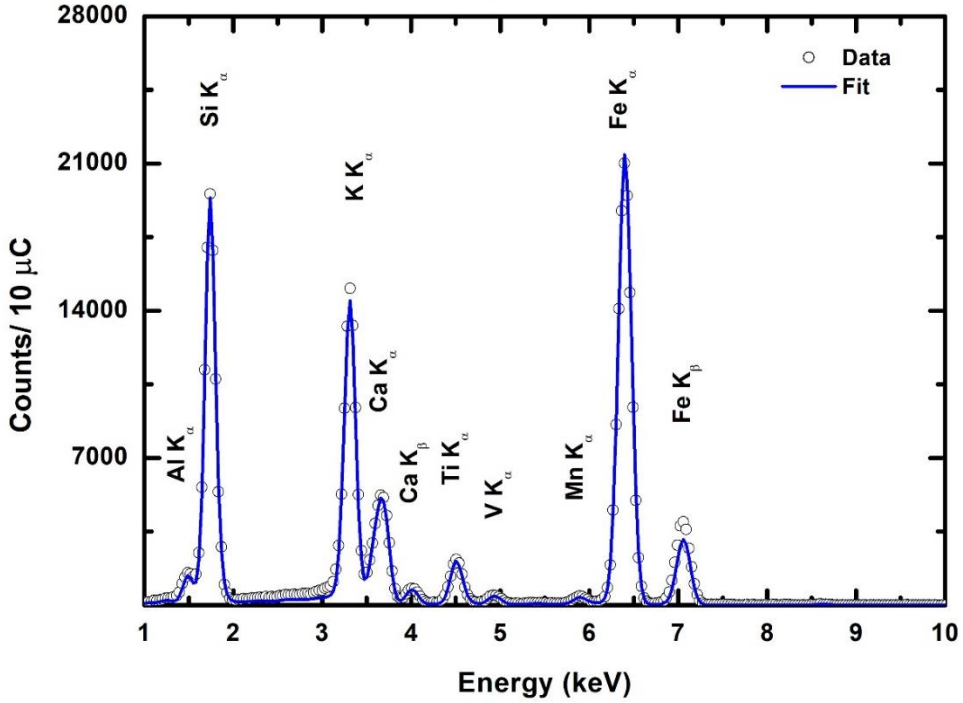

Figure 4.15: PIXE spectrum indicating the detected elements in the granodiorite sample.

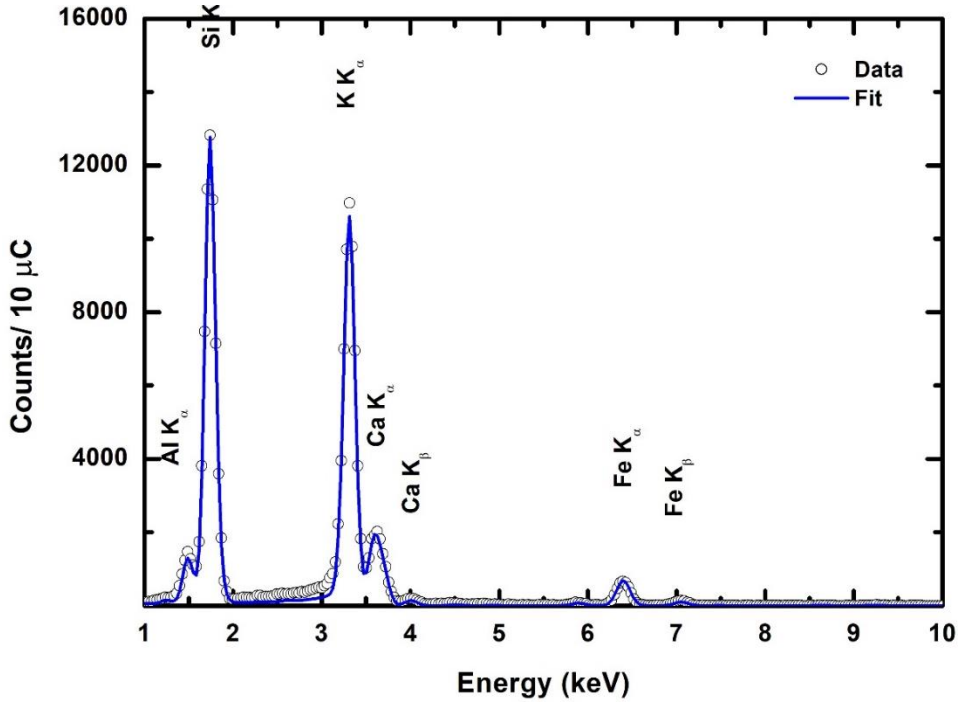

Figure 4.16: PIXE spectrum indicating the detected elements in the leucogranite sample.

4.2.2. Sample Characterization

In general, for rock samples, the intensities of the overall LIBS spectra were inconsistent from one sample to the other, this is due to, and amongst other factors the un-uniform sample composition (sample inhomogeneity), matrix effect and grain size. [38]. However, we can still compare the different samples qualitatively by comparing the existence of certain spectral lines in the spectra and quantitatively through the spectral lines normalised intensity. This was done by normalizing the spectra using the carbon atomic line at 247.87 nm.

4.2.2.1. Qualitative Characterization

Although it was very hard to differentiate qualitatively between samples because they nearly have the same matrix it was observed that the Fe ore sample had no magnesium lines.

Figure 4.17 demonstrates elemental differentiation between the samples from the LIBS spectra. As the spectral lines, Mg II at 280.3 nm and Mg I 285.22 nm lines are existing in all the samples except the iron ore sample. This is in good agreement with the geological theory the relatively low Mg content in Fe ore could be the result of Mg having a larger ionic radius and thus making it difficult to fit into the crystalline structure of the Fe ore; or it could be a simple reflection of lower concentrations of the Mg element in the carbonate protore [38].

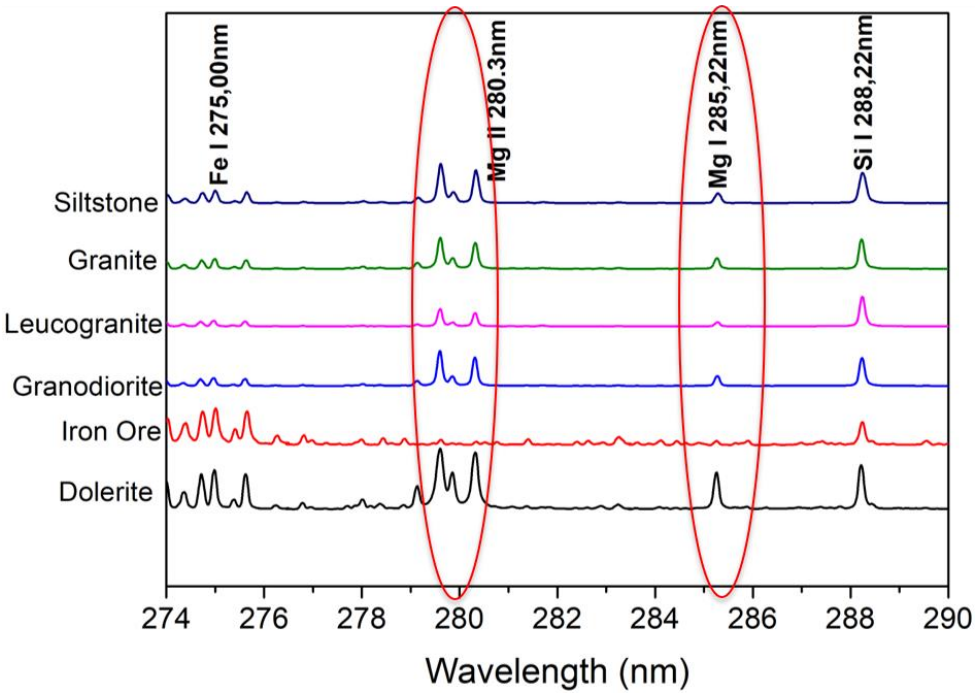

Figure 4.17: Comparative LIBS spectrum plotting emission signal intensity as a function of wavelength for all selected samples. Take note: the graphs have been shifted vertically for a clear demonstration.

4.2.2.2. Quantitative LIBS Characterization and the comparison with PIXE

To overcome the problem of sample inhomogeneity the spectra obtained from various positions were averaged. Figure 4.18 presents the LIBS normalised intensity of some elements, verified with PIXE results. This was done by following the trends of each element' (Fe, Mn, Ti, Ca, Si) concentration in 4 samples (Fe ore, granite, granodiorite and leucogranite).

LIBS measurements in fig. 4.18a, for Fe, show that the detection of Fe was higher in the Fe ore sample and lowest in Leucogranite; the same result was seen with PIXE (fig. 4.18b).

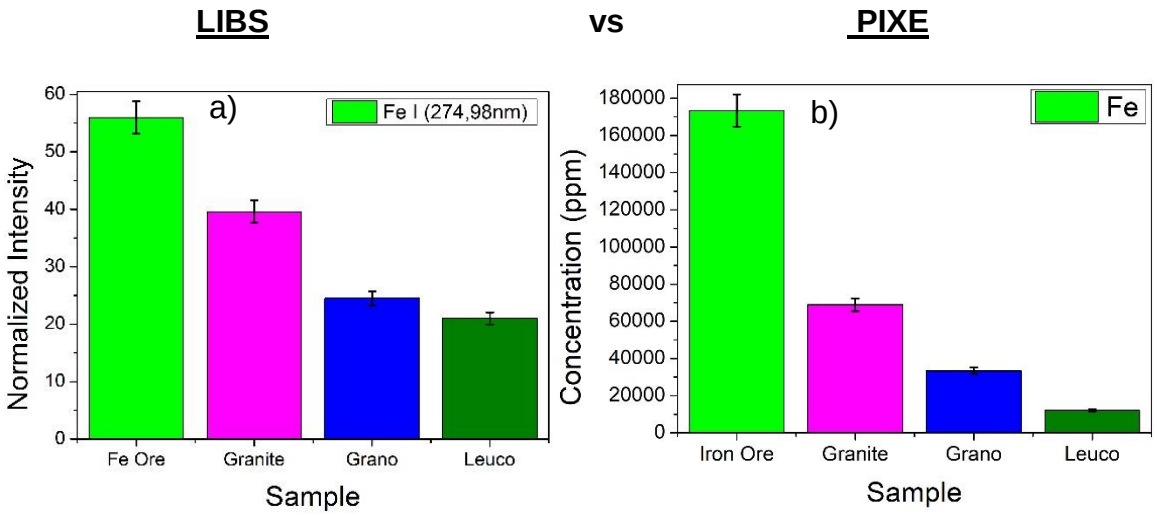

Figure 4.18(a; b): Normalized peak intensity ratios obtained for the measured rock samples, for element Fe using LIBS and PIXE.

Fig. 4.18(c, d) shows Mn results measured with LIBS and PIXE. The Mn trends were similar in the granite, granodiorite and the leucogranite sample. LIBS detected the presence of Mn in the Fe ore sample and with PIXE, Mn was not detected [68].

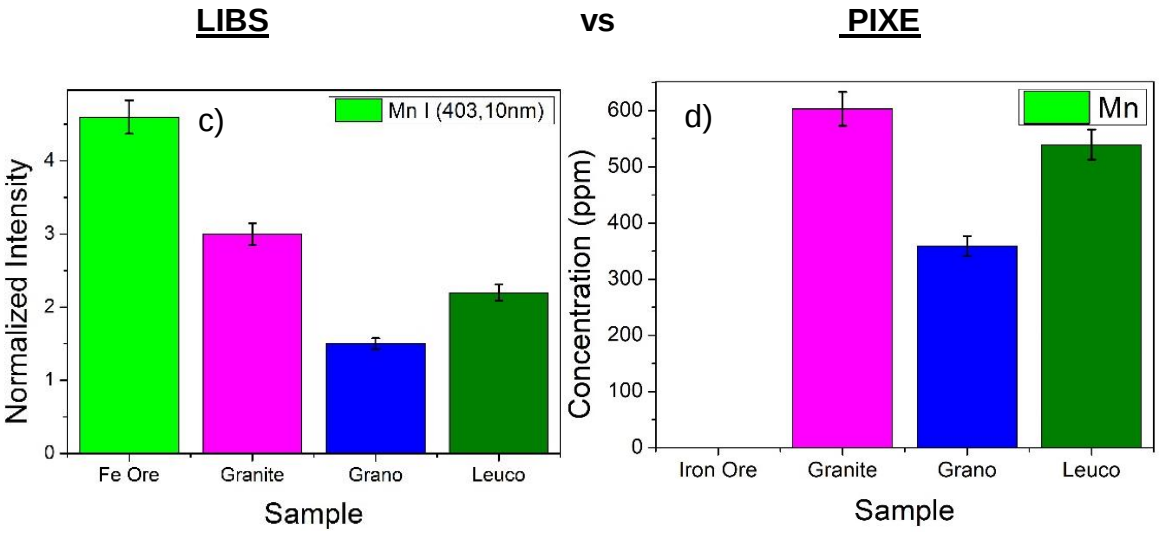

Figure 4.18 (c; d): Normalized peak intensity ratios obtained for the measured rock samples, for element Mn using LIBS and PIXE.

Figure 4.18e, shows Ti trends measured with LIBS, it was noticed that granite had a higher concentration of Ti compared to granodiorite and Fe ore did not show the line of Ti; measurements with PIXE (fig.4.18f) also confirmed that granite had higher concentration of Ti; with low concentration of Ti in the Fe ore sample. The absence of Ti in the Fe ore sample may be because the amount of Ti in the sample is below the detection limit of LIBS.

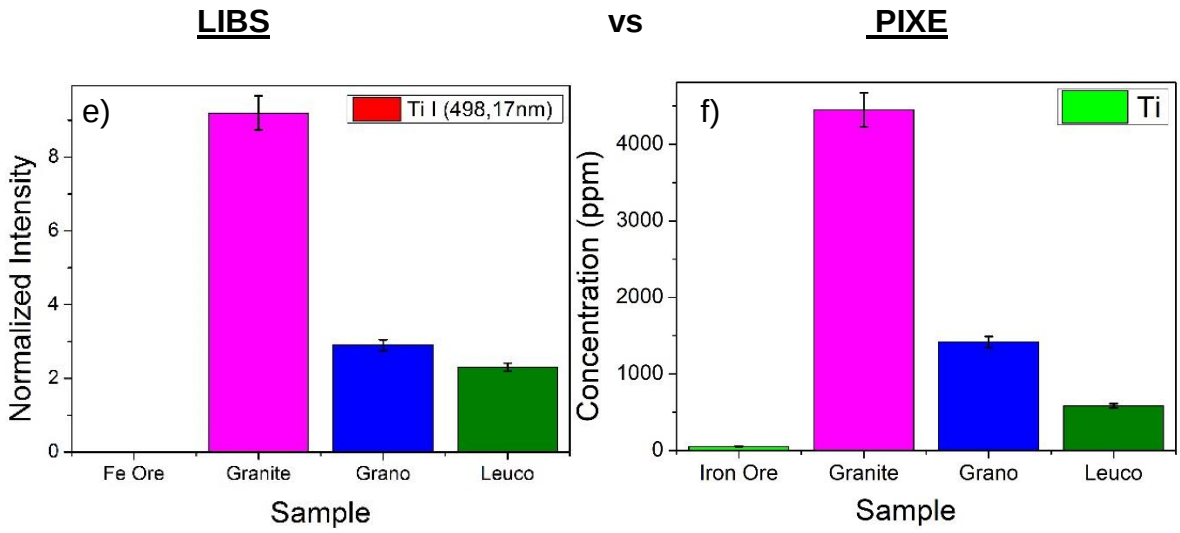

Figure 4.18(e; f): Normalized peak intensity ratios obtained for the measured rock samples, for element Ti using LIBS and PIXE.

Si is the most abundant element in the earth's crust and thus each igneous rock (except Fe ore) has a different Si composition. The granitic compositions (light coloured silicates: granites) have high silica content and are termed felsic rocks with silica (SiO2) content of about 72%, [69]. The PIXE results (fig. 4.18h) show that granodiorite has the highest Si content with granite showing the least and the LIBS results (fig. 4.18g) show different Si trends in the rocks. This could be the result of self-absorption of the element in the samples measured with LIBS.

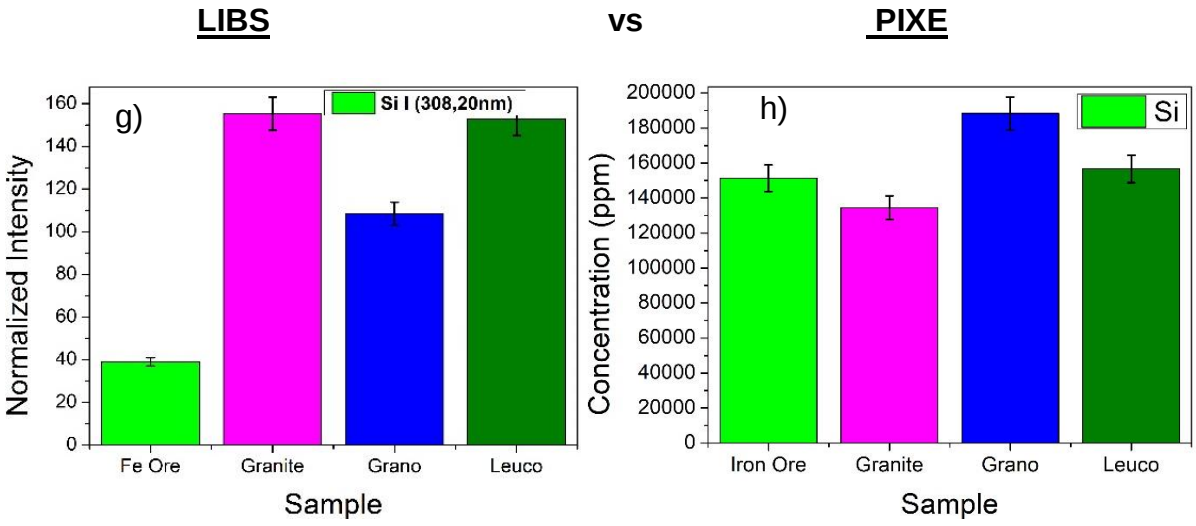

Figure 4.18(g; h): Normalized peak intensity ratios obtained for the measured rock samples, for element Si using LIBS and PIXE.

Granodiorite measured with the LIBS technique (fig. 4.18i) show higher concentrations of Ca while Fe ore shows the lowest concentration. Through megascopic (hand sample) descriptions, it was noticed that granodiorite had a dark green colour, this rock owes this colour to the fact that it contains more plagioclase (Ca and Na) feldspar than potassium feldspar and has darker minerals, thus the high content of Ca. The PIXE results (fig. 4.18j) agreed with the LIBS results with a high concentration of Ca in Granodiorite and low Ca concentration in the Fe ore sample [70].

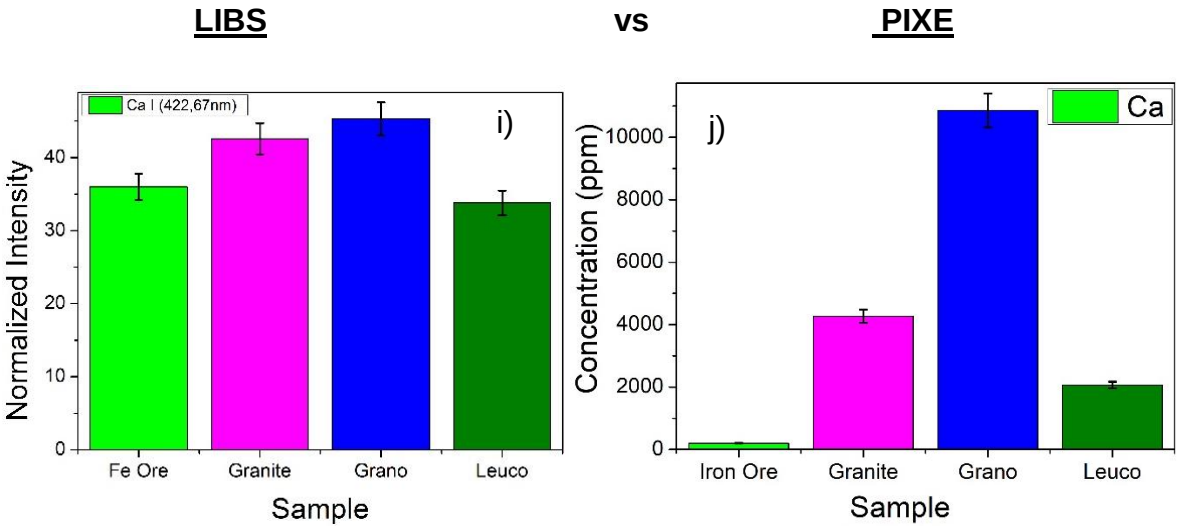

Figure 4.18(I; j): Normalized peak intensity ratios obtained for the measured rock samples, for element Ca using LIBS and PIXE.

In the case of elemental analysis, LIBS results were validated using PIXE and the results were in good agreement, thus proving that LIBS is an effective technique for elemental analysis of geomaterials and an effective technique for discriminating between the samples. The obtained results allowed the characterization of the samples.

4.2.3. Chemometrics

Traditional univariate and multivariate statistical methods have been used to model LIBS data. However, in this study one multivariate method was used to differentiate between geological materials: Principal component analysis (PCA); which was accomplished using the Origin Pro 2007 software package [1].

4.2.3.1. Principal Component Analysis (PCA)

PCA is a statistical method that is used in discovering chemical relationships within a complex spectral data set by performing linear regression in multidimensional space and is aimed to finding the principal components thus describing the major trends in the data set [71]. This analysis was also used by McManus et al (2008) [72] in combination with the LIBS spectra to identify Beryl from three beryl-bearing zones in Palermo before a successful experiment that provided a discriminating method between different specimens of Beryl.

In this study, PCA was used to differentiate and classify the LIBS data in terms of discriminant score plot. The set of LIBS measurements contained 6 samples of known origin. Figures 4.19 - 4.22 show the PC scores of the first two principal components (PC1 and PC2) for LIBS measurements. Plotting these scores makes it is likely to visualize grouping in the input data set which are indicative of the chemistry of the samples [73]. McMilan et al., (2014) [1], reports that the samples which plot close to one another on the PCA plot have similar compositions and that which plot far away from one another have different compositions.

Figure 4.19 represents all the six samples plotted together, the leucogranite sample (represented by the blue dots) is distinct from the rest of the samples; this observed dispersion in figure 4.19 may be the result of several factors but the most obvious is that: the leucogranite is a felsic rock meaning that it is a light - coloured granitic igneous rock, with almost no dark (mafic) minerals [74]. This feature sets the leucogranite aside from the rest of the rock samples. Whilst the other samples (Fe ore, granodiorite, leucogranite, granite and siltstone) are grouped in a single cluster (they overlap) which suggests that they are very similar in composition. Furthermore, the latter were divided into different clusters by successive PCA, where additional three PCAs were added to further discriminate between the samples according to their geological locations: (1) Dolerite and siltstone from Karoo Supergroup (Prince Albert Formation (Fm) in the

Eastern Cape, South Africa; (2) Granite (quartz) and iron ore from Gold and Iron exploration mines in the Gauteng Province, South Africa; (3) granodiorite and leucogranite from Karas region in Namibia.

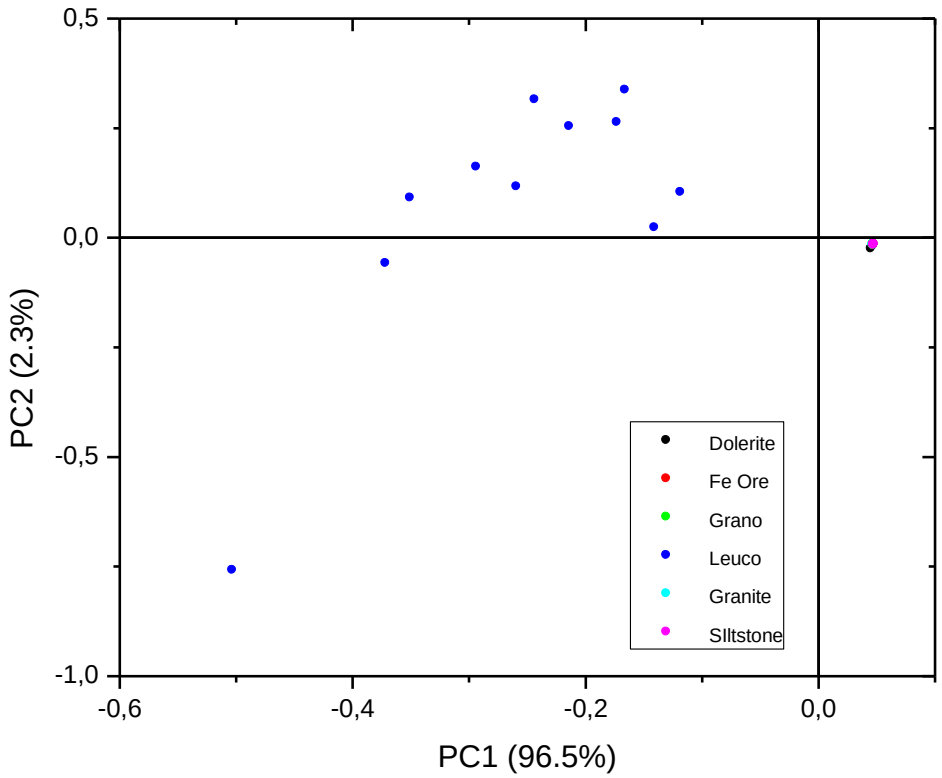

Figure 4.19: PCA scores plot for all the investigated samples.

The samples in Figures 4.20 (dolerite and Siltstone) and 4.21 (Fe ore and granite) are distinct from each other with an obvious dispersion between the samples (their compositional spaces do not overlap). Figure 4.22 (leucogranite and granodiorite) are distinct from each other; the leucogranite samples are well dispersed and the granodiorite plots in one cluster. It can be seen from the previous figures that LIBS-PCA (LIBS spectra analysed with principal component analysis) has illustrated the ability to differentiate between the samples with compositional similarities and the samples that deviate from the rest. The use of chemometrics in this study helped improve the discrimination of the samples using LIBS, it also illustrated the use of LIBS analysis in analytical geochemistry.

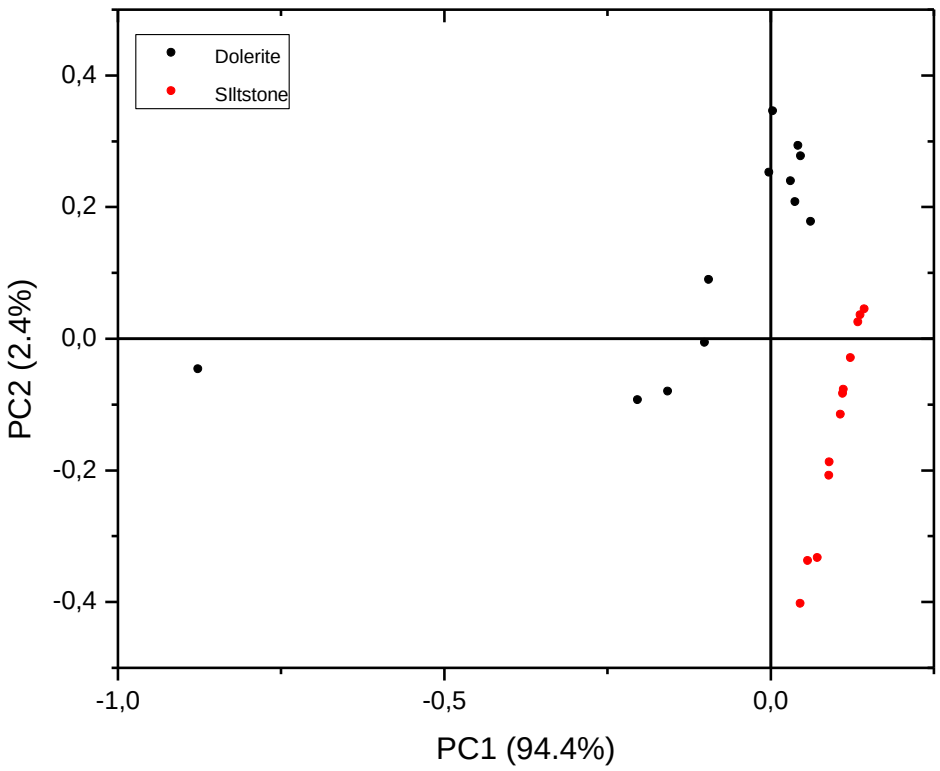

Figure 4.20: PCA scores plot for the dolerite and siltstone samples from the Karoo Supergroup (Prince Albert Formation, Eastern Cape, South Africa.

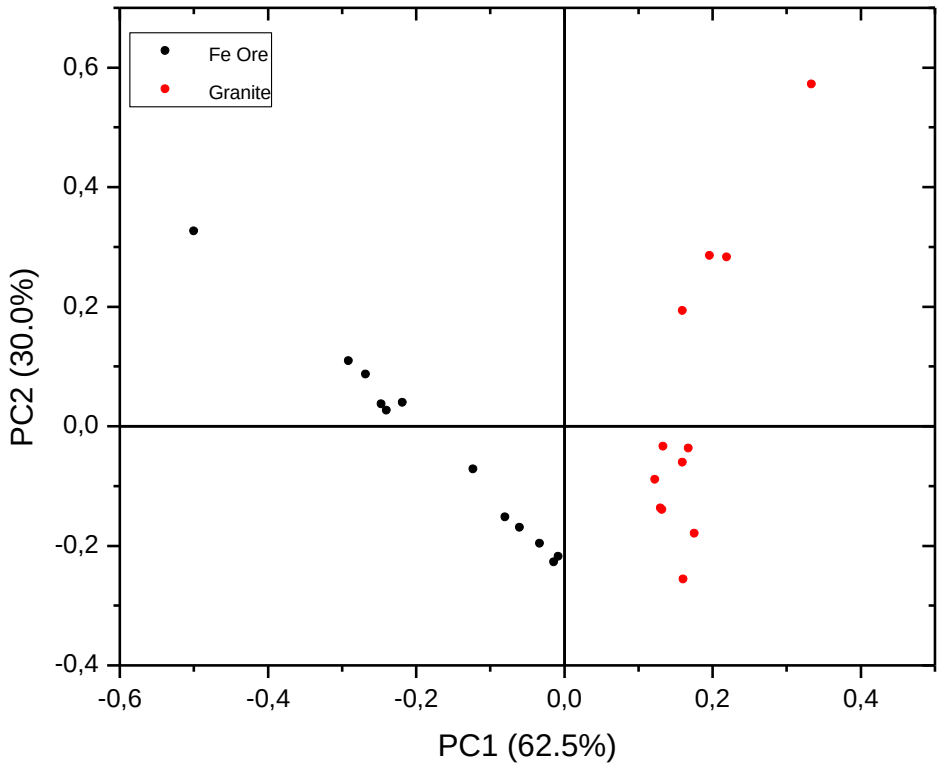

Figure 4.21: PCA scores plot for the Fe ore and Granite (quartz) samples from the Iron and gold exploration mines in Gauteng Province, South Africa.

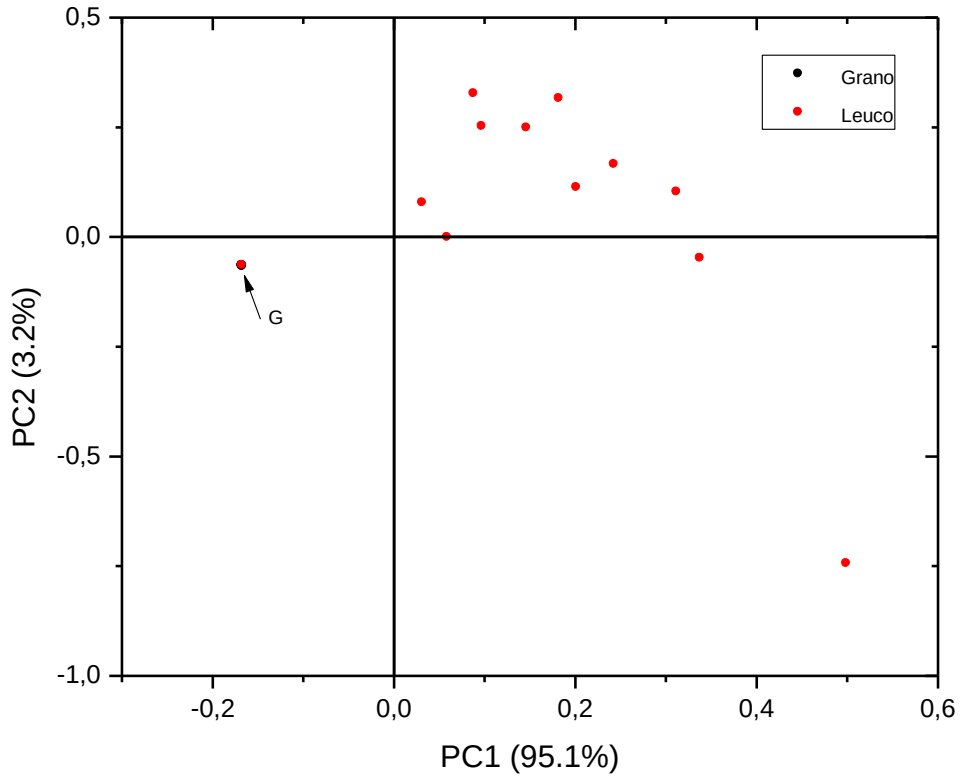

Figure 4.22: PCA scores plot for the granodiorite and leucogranite samples from the Karas region in Namibia.

4.3. Relative Hardness Estimation

4.3.1. Plasma Excitation Temperature

The feasibility of hardness measurement via the LIBS technique for geological samples was evaluated. This was done by measuring the value of the plasma excitation temperature (table 4.5) in 5 different samples (granodiorite, leucogranite, granite, Fe ore and Dolerite). The excitation temperature T_e was estimated from the emission intensity of the atomic Ti spectral lines listed in table 4.2. To do this, the theory requires that the plasma fulfils the LTE conditions (4.1.2). It has been attested that the differences in the hardness of the target materials can be associated with the changes in the values of the excitation temperature. [75]. Fig. 4.23., demonstrates the difference in the estimated relative hardness between the different samples. It was clear that; dolerite was the hardest being twice as hard as granodiorite followed by, Fe ore, granite and leucogranite. In this study, it was not possible to compare the LIBS results to the Vickers test results, because the samples were crushed under the tester tip. There was no feasible way to measure the hardness of the samples.

Table 4.5: The values of T_e, and sample density values.

Sample	T_e (K)	Sample Density (g/cm^3)
Granodiorite	2175.151	2.661
Leucogranite	3205.263	2.903
Granite	4514.535	2.661
Fe ore	5599.935	3.029
Dolerite	6386.92	3.123

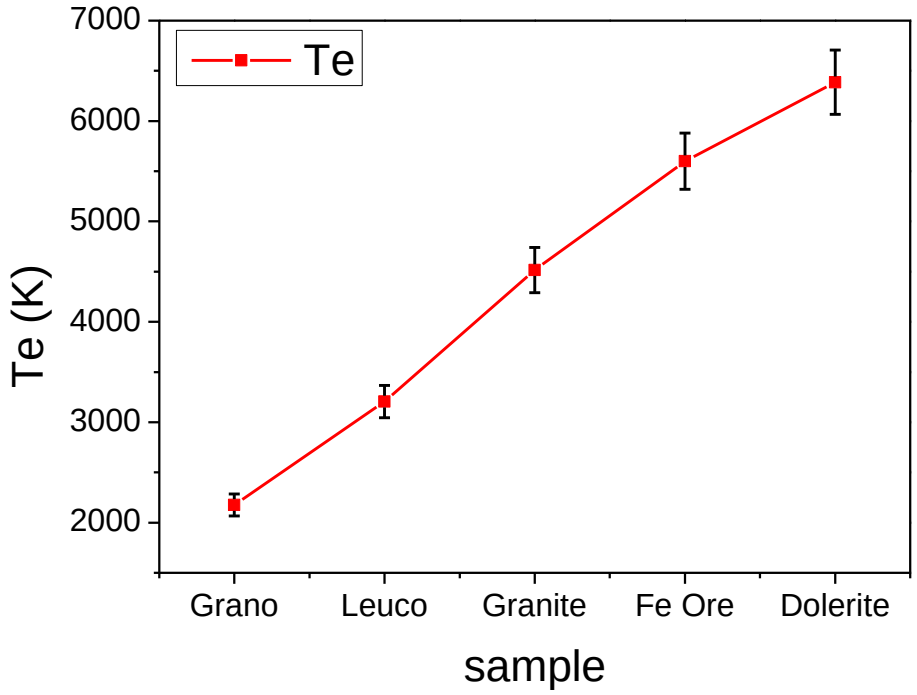

Figure 4.23: T_e for different samples

4.3.2. Plasma Excitation Temperature compared to Samples' Density

The hardness of a material is roughly correlative with the density of the material. To add to this statement several polymorphs have been studied and have been proved to show the same trend that the denser the material, the harder it is. This relationship has been proved to be logical, in the sense that the closer packing of atoms would contribute to the material having a greater density, thus allowing shorter bond lengths, which allows greater hardness [76].

The relationship between surface hardness of five geological samples (Granodiorite, granite, iron ore, leucogranite and dolerite) with the excitation temperature was investigated, with a comparison of the density of the samples. Plasma excitation temperature versus the density of the five samples is plotted in fig.4.24. The density of the samples was calculated by the equation:

$d = m/v$

Where m is the mass of the sample in grams (g) and v is the volume (cm^3) of the sample. Table 4.5 shows the sample densities.

As it is shown in figure 4.24 that T_e is directly proportional to the density of the samples which in turn is proportional to their hardness. [77], The direct proportionality between the plasma temperature and the density of the sample is acquired because of harder targets, the collisions in the plasma plume increase due to strong repulsive forces. This result is like the result obtained by [78] where they applied LIBS for the analysis of Ti-based alloys, the results demonstrated a linear relationship between sample surface hardness and plasma temperature. Pilkington, et al., 2015 [75] also applied LIBS for the analysis of surface hardness measurements, the results demonstrated the possibility to relate the hardness value to the plasma temperature.

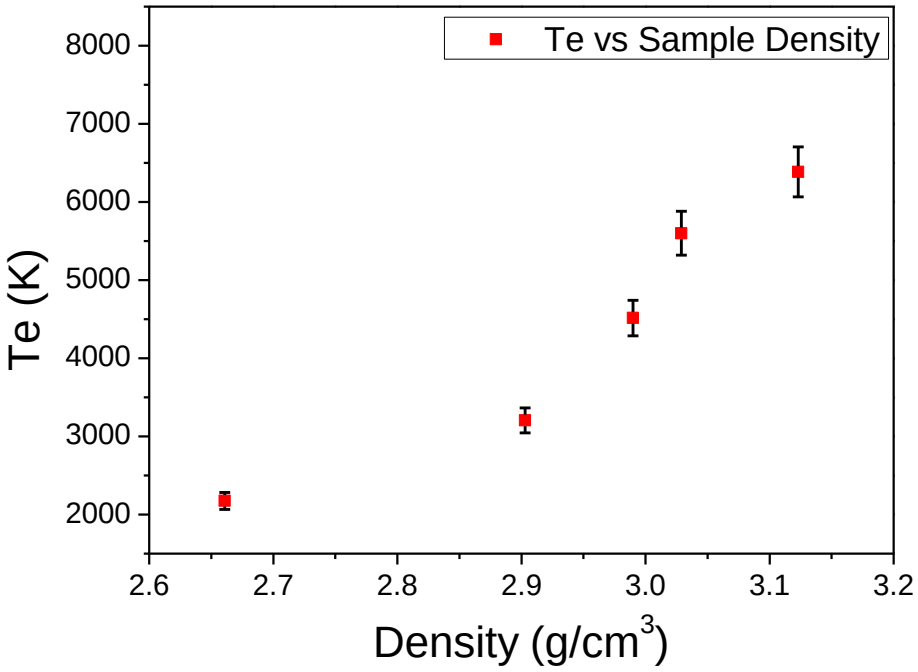

Figure 4.24: Excitation temperature vs samples density for different samples (Panya panya, 2017).

LIBS with its advantages as an elemental technique made it possible to estimate the hardness of geological samples. We have shown that plasma excitation temperature displays a linear dependence on samples' hardness. From the results of this study is envisaged that LIBS demonstrate the feasibility for estimating the relative hardness of geological samples. Additionally, LIBS should not only be considered as a chemical analytical technique but also be recognised as a flexible technique capable of measuring the surface hardness.

SUMMARY AND CONCLUSION

LIBS is emerging as a multipurpose technique for geological studies due to its many advantages, particularly easy and fast analysis with little or no sample preparation required.

The main aim of this master dissertation has been to use Laser-Induced Breakdown Spectroscopy (LIBS) as a fast, real-time analytical technique to compositionally differentiate between geological samples and to measure their hardness properties. With the objective to define the optimum LIBS experimental conditions and parameters essential for the precision of the results, to investigate the elemental composition of samples as well as to estimate the relative hardness of the samples by measuring the electron temperature and the density of the samples.

The investigated experimental condition was the time delay. A detailed discussion of the experimental condition revealed that delay time at 1000 ns was the best point for time delay when a 50 mJ laser pulse hit the surface of the sample. The analysed samples were rock fragments collected from the field. Spectral lines that are characteristic of the major components of the earth's crust (including Si, Al, Fe, Ca, Mg, Na, and Ti) were measured. It was found that LIBS was able to identify the existence of the elements in the rock samples. Also, qualitatively it was able to differentiate the iron ore sample from the other samples due to the absence of the magnesium in the iron ore. This is also agreeing with the geological concept which indicates that an iron ore sample contains little or no Mg content owing this to the fact that Mg has a larger ionic radius and therefore does not fit into the crystalline structure of the Fe ore. Quantitatively, LIBS was also able to differentiate between the samples based on the amounts of every element in the samples. The LIBS results were confirmed using Particle Induced X-ray Emission (PIXE) where the LIBS results were found to be in a good agreement with the PIXE results. To get better differentiation between the rock samples LIBS spectra for all the samples were correlated statistically using Principle Component Analysis (PCA). It was found that using the PCA analysis; it is possible to make a fine and quick differentiation between samples even those from the same area.

For relative hardness quantification, the value of the plasma excitation temperature (T_e) and the density of the samples were measured in the different samples. It has been shown that plasma excitation temperature displays a linear dependence on samples' hardness. From the results of this study, LIBS has demonstrated the feasibility for estimating the relative hardness of geological samples

From all the results presented in this work, we can see that LIBS can be used for both analytical analysis and hardness measurement of rock samples simultaneously without the need for huge sample preparations or complicated technical procedures.

REFERENCES

[1] N. McMillan, S. Rees, K. Kochelek and C. McManus, “Geological Applications of Laser-Induced Breakdown Spectroscopy,” *Geostandards and Geoanalytical Research,* vol. 38, pp. 329-343, 2014.

[2] D. Pace, N. Gabriele, M. Garcimuno, C. D'Angelo and D. Bertuccelli, “Anlysis of Minerals and Rocks by Laser-Induced Breakdown Spectroscopy,” *Spectroscopy Letters,* vol. 44, pp. 399-411, 2011.

[3] R. Harmon, F. De Lucia, C. McManus, N. McMillan, T. Jenkins, M. Walsh and A. Miziolek, “Laser-Induced Breakdown Spectroscopy - An Emerging Chemical Sensor Technology For Field Portable , Real time Geochemical, Mineralogical and Environmental Applications,” *Application Geochemistry,* pp. 730-747, 2006.

[4] C. Mcmanus, N. McMillan, R. Harmon and R. Whitemore, “The Use of Laser-Induced Breakdown Spectroscopy (LIBS) in the Determination of Gem Provenance: Beryls,” *Applied Optics,* vol. 47, pp. G72-G79, 2008.

[5] R. Harmon, J. Remus, N. McMillan, C. McManus, L. Collins, J. Gottfried Jr, F. DeLucia and A. Miziolek, “LIBS Analysis of Geomaterials: Geochemical Fingerprinting for the Rapid Analysis and Discrimination of Minerals,” *Applied Geochemistry,* vol. 24, pp. 1125-1141, 2009.

[6] D. Cremers and L. Radziemski, “History and Fundamentals of LIBS,” in *Laser Induced Breakdown Spectroscopy(LIBS): Fundamentals and Applications*, A. Miziolek and V. &. I. Schechter, Eds., United States, Cambridge University Press, 2006, pp. 1-39.

[7] D. Alvey, K. Morton, R. Harmon, J. Gottfried, J. Remus, M. Collins and M. Wise, “Laser-Induced Breakdown Spectroscopy- Based Geochemical Fingerprinting for the Rapid Analysis and descrimination of minerals: The Example of Garnet,” *Applied Optics,* vol. 49, pp. 168-180, 2010.

[8] M. Kasem and M. Harith, “Laser-Induced Breakdown Spectroscopy in Africa,” *Journal of Chemistry,* pp. 1-10, 2015.

[9] A. Miziolek, V. Palleschi and I. Schechter, Laser-Induced Breakdown Spectroscopy (LIBS) Fundamentals and Applications, Cambridge, UK: Cambridge University Press, 2006.

[10] S. Thakur and J. Singh, “Fundamentals of Laser Induced Breakdown Specroscopy,” India, 2007.

[11] NIST, NIST Elecronic Data Base for Neutral and Ionized Elements, Avaialable at https://physics.nist.gov/PhysRefData/ASD/lines_form.html, Accessed 6 October 2016.

[12] D. Hahn and N. Omenetto, “Laser-Induced Breakdown Spectroscopy (LIBS), Part I: Review of Basic Diagnostics and Plasma- Particle Interactions:Still-Challenging Issues Within the Analytical Plasma Community,” *Applied Spectroscopy,* pp. 335-366, 2010.

[13] D. Hahn and N. Omenetto, “Laser-Induced Breakdown Spectroscopy (LIBS), Part II: Review of Instrumental and Methodological Approaches to Material Analysis and Applications to Different Fields,” *Applied Spectroscopy,* pp. 347-419, 2011.

[14] F. Anabitarte, A. Cobo and J. Lopez-Higuera, “Laser-Induced Breakdown Spectrosopy: Fundamentals, Applications and Challenges,” *ISRN Spectroscopy,* vol. 2012, pp. 1-12, 2012.

[15] D. Cremers and L. Radziemski, Laser-Induced Breakdown Spectroscopy, John Wiley & Sons, 2013.

[16] A. Miziolek, V. Palleschi and I. Schechter, Laser-Induced Breakdown Spectroscopy (LIBS)- Fundamentals and Applications, New York: Cambridge Univeristy Press, 2006.

[17] K. Tsuyuki, S. Miura, N. Idris, K. Hendrik, K. Kurniawam, T. Lie and K. Kagawa, “Measurement of Concrete Strength Using the Emission Intensity ratio between Ca(II) 396.8 and Ca(I) 422.6 in a Nd:YAG Laser-Induced Plasma,” *Applied Spectroscopy,* vol. 60, pp. 61-64, 2006.

[18] Z. Abdel-Salam, A. Galmed, E. Tognoni and M. Harith, “Estimation of Calcified Tissue Hardness via Calcium and Magnesuim Ionic to Atomic Line Intensity in Laser Induced Breakdwon Spectra,” *Spectrochimica Acta Part B,* vol. 62, pp. 1343-1347, 2007.

[19] R. Noll, “Laser Induced Breakdown Spectroscopy,” in *Laser Induced Breakdown Spectroscopy (Fundamentals and Applications)*, Germany, Springer, 2002, pp. 7-15.

[20] H. Bauer, F. Leis and K. Niemax, “Laser- Induced Breakdown Spectroscopy with an echelle spectrometer and intensified charge coupled device detection,” *Spectrochimica Acta A,* pp. 1815-1825, 1998.

[21] A. Ambushe, A. du Plessis and R. McCrindle, “Laser-Induced Breakdwon Spectroscopy and Inductively Coupled Plasma-Mass Spectrometry for Determination of Cr in Soils from Brits District, South Africa,” *Bull. Chemical Society of Ethiopia,* vol. 29, pp. 357-366, 2015.

[22] J. Vadillo and J. Laserna, “Chemical Imaging of surfaces Using LIBS,” in *Laser-Induced BreakdownSpectroscopy (LIBS): Fundamentals and Applications*, United States, Cambridge University Press, 2006, pp. 254-281.

[23] C. Davies, H. Telle, D. Montgomery and R. Corbett, “Quantitative Analysis Using Remote Laser- Induced Breakdown Spectroscopy (LIBS),” *Spectrochima Acta B,* vol. 50, pp. 1059-1075, 1995.

[24] A. Knight, N. Scherbarth, D. Cremers and M. Ferris, “Characterization of Laser-Induced Breakdown Spectroscopy (LIBS) for Application to Space Exploration,” *Applied Spectroscopy,* vol. 54, pp. 331-340, 2000.

[25] A. Eppler, D. Cremers, D. Hickmott, M. Ferris and A. Koskelo, “Matrix Effects in the Detection of Pb and BA in Soils Using Laser-Induced Breakdown Spectroscopy,” *Applied Spectroscopy,* vol. 50, pp. 1175-1181, 1996.

[26] M. Kasem, R. Russo and M. Harith, “Influence of Biological Degradation and Environmental Effects on the Interpretation of Archeological Bone Samples with LIBS,” *Journal of Analytical Atomic Spectrometry,* vol. 26, pp. 1733-1739, 2011.

[27] N. Idris, K. Tsuyuki, S. Miura, K. Kurniawan and K. Kagawa, “Prelim Laser-Induced Plasma Spectroscopy (LIBS) Study Towards Quick Inspection of Building Quality in Disaster Vulnerable Regions,” in *5th Annual International Workshop & Expo on Sumatra Tsunami Disaster & Recovery*, 2010.

[28] A. Galmed, A. Kasem, H. Von Bermann and M. Harith, “The Effect of Normalization for depth Profiling LIPS Experiment,” in *AIP Conference*, 2011.

[29] V. Singh, V. Kumar and J. Sharma, “Importance of Laser-Induced breakdown Spectroscopy for Hard Tissues (Bone and Teeth) and Other Calcified Tissue Materials,” *Lasers in Medical Science,* vol. 30, pp. 1763-1778, 2015.

[30] L. Torrisi, F. Caridi, Giuffrida, A. Torrisi, G. Mondio, T. Serafino, M. Caltabiano, E. Castrizio, E. Paniz and A. Salici, “LAMQS Analysis Applied to Ancient Egyptian Bronze Coins,” *Nuclear Instruments and Methods in Physics Research,* vol. 268, pp. 1657-1644, 2010.

[31] L. Caneve, A. Diamanti, F. Grimaldi, G. Palleschi, V. Spizzichino and F. Valentini, “Analysis of Fresco by Laser-Induced Breakdown Spectroscopy,” *Spectrochimica Acta Part B,* vol. 65, pp. 702-706, 2010.

[32] A. Whitehouse, J. Young, I. Botheroyd, S. Lawson, C. Evans and J. Wright, “Remote Material Analysis of Nuclear Power Station Steam Generator Tubes by Laser-Induced breakdwon Spectroscopy,” *Spectrochimica Acta Part B,* vol. 56, pp. 821-830, 2001.

[33] N. Rai and A. Rai, “LIBS- An Efficient approach for the Determination of Cr i Industrial Wastewater,” *Journal of Hazardous Materials, vol. 50, no.3,* vol. 150, pp. 835-838, 2008.

[34] J. Kowalczyk, J. Perkins, J. Kaneshiro, N. Gaillard, Y. Chang, A. DeAngelis, S. Mallory, D. Bates and E. Miller, “Measurement of the Sodium Concentration in CIGS Solar Cells via Laser-Induced Breakdown Spectroscopy,” in *In Proceedings of hte 35th IEEE Photovoltaic Specialists Conference (PVSC' 10)*, Hanolulu, Hawaii, June 2010.

[35] S. Qiao, Y. Ding, D. Tian, L. Yao and G. Yang, “A Review of Laser-Induced Breakdown Spectroscopy for Analysis of Geological Materials,” *Applied Spectroscopy,* vol. 50, pp. 1-26, 2015.

[36] D. Death, A. Cunningham and P. L.J., “Multi-Element and Mineralogical Analysis of Mineral Ores Using Laser-Inducd Breakdown Spectroscopy and Chemometric Analysis,” *Spectrochimica Acta Part B,* vol. 64, pp. 1048-1058, 2009.

[37] D. Roberts, A. du Plessis, J. Steyn, L. Botha, S. Pityana and L. Berger, “An Investigation of Laser-Induced Brekadown Spectroscopy for Use as a Control in the Laser Removal of Rock from Fossils found at the Malapa Hominin Site, South Africa,” *Spectrochimica Acta Part B,* vol. 73, pp. 48-54, 2012.

[38] A. Kiros, V. Lazic, G. Gigante and A. Gholap, “Analysis of Rock Samples collected From Rock Hewn Churches of Lalibela, Ethiopia using Laser-Induced Breakdwon Spectrosopy,” *Journal of Archaeological Science,* vol. 40, pp. 2570-2578, 2013.

[39] C. Mcmanus, N. McMillan, R. Harmon, R. Whitemore, F. DeLucia and A. Miziolek, “The Use of Laser- Induced Breakdown Spectroscopy (LIBS) in the Determination of Gem Provanance,” *Applied Opt,* pp. 72-79, 2008.

[40] M. Gondal, T. Hussain, Z. Yamani and M. Baig, “Detection of Heavy Metals in the Arabian Crude Oil Residue Using Laser-Induced Breakdown Spectroscopy,” *Talanta 69,* vol. 69, pp. 1072-1078, 2006.

[41] S. Wold, “Chemometrics; What Do We Mean With it, and What do we Want From It?,” *Chemometrics and Intelligent Laboratory Systems,* vol. 30, pp. 109-115, 1994.

[42] H. Verma, “X-ray Fluorescence (XRF) and Particle Induced X-ray Emission (PIXE). XRF, Mössbauer, XPS, NAA and Ion-Beam Spectroscopic Techniques,” in *Atomic and Nuclear Analytical Methods*, Springer, 2007, pp. 1-91.

[43] B. Castle, K. Talabardon, B. Smith and J. Winefordner, “Variables Influencing the Precision of Laser- Induced Breakdown Spectroscopy Measurements,” *Applied Spectroscopy. ,* vol. 52, pp. 649-657, 1998.

[44] B. Fisher, H. Johnsen, S. Buckley and D. Hahn, “Temporal Gating for the Optimization of Laser-Induced Breakdown Spectroscopy Detection and Analysis of Toxic Metals,” *Applied Spectroscopy,* vol. 55, pp. 1312-1319, 2001.

[45] M. Martin and M. Cheng, “Detection of Chromium Aerosol Using Time-Resolved Laser-Induced Plasma Spectroscopy,” *Applied Spectroscopy,* vol. 54, pp. 1279-1285, 2000.

[46] A. Galmed and M. Harith, “Temporal Follow Up of the LTE Conditions in Aluminum Laser-Induced Plasma at Different Laser Energies,” *Applied Physics B,* vol. 91, pp. 651-660, 2008.

[47] L. Cabalin and J. Laserna, “Experimental Determination of Laser-Induced Breakdown Spectroscopy Threshold of Metals Under Nanosecond Q-Switched Laser Operation,” *Spectrochimica Acta B,* vol. 53, pp. 723-730, 1998.

[48] E. Harby and A. Olodia, “From Ptolemaic to Modern Inked Linen via Laser-Induced Breakdown Spectroscopy (LIBS),” *Analytical Methods ,* vol. 5, pp. 3114-3121, 2013.

[49] G. Bekefi, C. Deutsch and B. Yaakobi, “Spectroscopic Diagnostics of Laser,” in *Principles of Laser Plasmas*, New York, Wiley Intersciences, 1994.

[50] A. Galmed and M. Harith, “Temporal Follow Up of the LTE Conditions i Alluminium Laser- Induced Plasmas at Different Laser Energies,” *Applied Physics B,* vol. 91, pp. 651-660, 2008.

[51] G. Senesi, P. Benedetti, G. Cristoforetti, S. Legnaioli and V. Pelleschi, “Hydrogen Balmera Line Behavior in Laser- Induced Breakdown Spectroscopy Depth Scans of Au, Cu, Mn, Pb Targetsi Air,” *Spectrochimica Acta Part B ,* vol. 65, pp. 557-564, 2010.

[52] P. W. J. M. Boumans, “Exciteaton Phenomenona and Temperature Measurements,” in *Theory of Spectrochemical Excitation*, London, Hilger and Watts, 1966.

[53] W. Lochte-Holtgreven, in *Plasma Diagnostics*, New York, Wiley Interscience, 1964.

[54] H. Griem, Plasma Spectroscopy, McGraw Hill, New York, 1964.

[55] R. McWhirter, “Spectral Intensities,” in *Plasma Diagnostic Techniques*, New York, Academic, 1965.

[56] C. Fabre, M. Boiron, J. Dubessy, A. Chabiron, R. Charoy and T. Crespo, “Advances in Lithium Analysis in Solids By Means of Laser-Induced Breakdown Spectroscopy: An Exploratory Study,” *Geochemicha et Cosmochimica Acta,* vol. 66, pp. 1401-1407, 2002.

[57] J. Remus, J. Gottfried, R. Harmon, A. Draucker, D. Baron and R. Yohe, “Arcehological Applications of Laser-Induced Breakdown Spectrocopy: An Example of the Coso Volcanic Field. Califonia, Using Adanced Statistical Signal Proccessing,” *Appied Optics,* vol. 49, pp. C120-C131, 2010.

[58] A. Striganove and N. Sventitski, Table of Spectral Lines of Neutral and Ioniszed Atoms, New York, 1968.

[59] NIST, NIST Electronic Database for Neutral and Ionized Elements, Avaialable at https://physics.nist.gov/PhysRefData/ASD/lines_form.html, Accessed 05 April 2017.

[60] L. Railsback, “An Earth Scientist Periodic Table of the Elements and Their Ions,” *Geology,* vol. 39, pp. 373-740, 2003.

[61] B. Yardley and R. Bodnar, “Fluids in the Continental Crust,” *Geochemical perspective,* vol. 3, pp. 1-127, 2014.

[62] M. Kasem and M. Harith, “Laser-Induced Breakdown Spectroscopy in Africa,” *Journal of Chemistry,* pp. 1-10, 2015.

[63] K. Malmqvist, “Biological and Medical Applications,” in *Particle Induced X-ray Emission Spectrometry*, New York, Wiley, 1995.

[64] V. Kennedy, A. Augusthy, K. Varier, S. Magudapathy, V. Panchapakesan, V. Vijayan and K. Nair, “Trace Metal Distribution Studies in River Water by PIXE,” *Nucl. Instr and Meth B,* vol. 150, pp. 277-281, 1999.

[65] V. Kennedy, G. Stephenson, W. Trompetter, B. Barry and A. Markwitz, “Trace Element Distribution Studies in River Water by PIXE,” *Nucl. Instr and Meth in Phys. Res. ,* vol. 258, p. 435, 2007.

[66] J. Maxwell, W. Teesdale and J. Campbell, “The Guelph GUPIX Software Package IT,” *Nucl. Instr and Meth B ,* vol. 95, p. 407, 1995.

[67] S. Johannson and K. Bartfoot, PIXE: A Novel Technique for Elemental Analysis, Chichester: Wiley, 1988.

[68] C. Ryan, F. Clayton, W. Griffin, S. Sie and D. Cousens, “Snip, A Statistical - Sensitive Background Treatment for the Quantitative Analysis of PIXE Spectra in the Geoscience Applications,” *Nuclear Instruments and Methods in Physics Research B34,* pp. 396-402, 1998.

[69] J. Walsh, “Determination of Silica in Rocks and Minerals by a Combined Gravimetric and Atomic - Absorption Spectrophotometric Procedure,” *Analyst,* vol. 1210, pp. 51-54, 1977.

[70] D. Johnson, P. Hooper and R. Conrey, “XRF Analysis of Rocks and Minerals for Major and Trace Elements On a Single Low Dilution Li-tetraborate Fused Bead,” *Internatuonal Centre for Diffraction Data,* vol. 41, pp. 843-867, 1999.

[71] J. Gottfried, R. Harmon, F. De Lucia and A. & Miziolek, “Multivariate Analysis of Laser-Induced Breakdown Spectroscopy Chemical Signatures for Geomaterial Classification,” *Spectrochimica Acta B,* pp. 1009-1019, 2009.

[72] C. McManus, N. McMillan, R. Harmon and &. W. R.C., “Use of Laser-Induced Breakdown Spectroscopy in the Determination of Gem Provenance: Beryls,” *Applied Optical Spectroscopy Vol 47,* pp. G72-G79, 2008.

[73] D. Death, A. Cunningham and L. Pollard, “Multi-Elementand Mineralogical Analysis of Mineral Ores Using Laser- Induced Breakdown Spectroscopy and Chemometric Analysis,” *Spectrochima Acta Part B Vol 64,* pp. 1048-1058, 2009.

[74] M. Ibrahim, A. Hussein, A. Osman and I. Ibrahim, “Uranuin Geochemistry in Paraluminous Leucogranites of Wadi El-Shallal Area, Sinai, Egypt,” *Journal of Earth Science ,* vol. 12, pp. 17-37, 2000.

[75] R. Pilkington, J. Astin and J. Cowpe, “Application of Laser-Induced Breakdown Spectroscopy for Surface Hardness Measurements,” *Spectroscopy Europe ,* vol. 27, pp. 13-15, 2015.

[76] L. Railsback, “Some Fundamentals of Mineralogy and Geochemistry,” University of Georgia, Athens, Georgia, 2006.

[77] J. Cowpe, R. Moorehead, D. Moser, J. Astin and S. Karthikeyan, “Hardness Estimation of Bio-Ceramics Using Laser-Induced Breakdown Spectroscopy,” *Spectrochimica Acta PArt B Atomic Spectroscopy,* vol. 66, pp. 290-294, 2011.

[78] O. Mohamed, G. A.H. and N. O.A, “Determination of Surface Hardness of Ti-Based Alloys via Laser-Induced Breakdown Spectroscopy,” *Arab Journal of Nuclear Science and Applications,* vol. 50, pp. 142-155, 2017.

APPENDIX

Papers published (Appendix 1)

- ✓ S.N. Panya panya, A.H. Galmed, M. Maaza, B.M. Mothudi, M.A. Harith, J. Kennedy, “Laser-Induced Breakdown Spectroscopy (LIBS) on Geological Samples: Compositional Differentiation”, Materials Research Society 2017, Vol. 3, pp 1969-1983, 2018. DOI: 10.1557/adv.2018.401

Papers presented at conferences

- ✓ **2017:** Poster Presentation on ‘Laser Induced Breakdown Spectroscopy on Geological samples’ at the 9th International Conference of the African Materials Research Society (11-14 December 2017), Gaborone, Botswana.